

THE ORIGIN AND STRUCTURE OF EASTERLY WAVES  
IN THE LOWER TROPOSPHERE OF NORTH AFRICA

by

ROBERT W. BURPEE

A.B. Harvard University (1963)

S.M. Massachusetts Institute of Technology (1966)

SUBMITTED IN PARTIAL FULFILLMENT OF THE  
REQUIREMENTS FOR THE DEGREE OF DOCTOR OF PHILOSOPHY

at the

MASSACHUSETTS INSTITUTE OF TECHNOLOGY

January 1971



Signature of Author . . . . .  
Department of Meteorology, 15/ January 1971

Certified by . . . . .  
Thesis Supervisor

Accepted by . . . . .  
Chairman, Departmental Committee on Graduate Students

THE ORIGIN AND STRUCTURE OF EASTERLY WAVES IN THE  
LOWER TROPOSPHERE OF NORTH AFRICA

by

Robert W. Burpee

Submitted to the Department of Meteorology on January  
15th, 1971 in partial fulfillment of the requirements  
for the degree of Doctor of Philosophy.

ABSTRACT

This study investigates the origin and structure of easterly waves which form in the lower troposphere of North Africa and have a periodicity of 4-5 days. From June to early October these waves account for approximately half of the tropical cyclones which form in the Atlantic and may be a factor in the development of tropical storms in the eastern Pacific.

Spectral analysis of five years of upper-air data shows that African waves produce a spectral peak of the meridional wind at periods of 4-5 days with a maximum amplitude of 1-2 m/sec near 700 mb. The waves normally originate between Khartoum (32°E) and Ft. Lamy (15°E) and affect a greater depth of the atmosphere as they propagate westward. The wave axis tilts eastward with height up to 700 mb and tilts westward above this level. Cross-spectrum analysis of the wind and height fields reveals that the waves are geostrophically balanced. The thermal wind equation indicates that the mean temperature amplitude is too small to identify by spectral methods with existing data. In east-central Africa convection associated with the waves is not well developed, but convection becomes better organized as the waves propagate westward. Even in West Africa, however, there is no preferred pattern of maximum convection relative to the trough axis.

Wind statistics at stations flanking the mountains in Ethiopia indicate that these mountains are not the cause of the easterly waves. The waves are directly related to the mid-tropospheric easterly jet which is found above the surface baroclinic zone to the south of the Sahara. The mean zonal current in this region is barotropically unstable in the middle troposphere during the same season that African waves are observed and it is within this zone that the disturbances form. The waves transport easterly momentum away from the mid-tropospheric jet and the jet is maintained by a thermally direct, ageostrophic meridional circulation. While the effect of baroclinic terms cannot be determined, the average surface temperature gradient of 10°C in 10° latitude is so large that baroclinic processes are quite likely important.

Thesis Supervisor: Frederick Sanders  
Title: Professor of Meteorology

## Table of Contents

1. Introduction	4
2. Description of North African Summer Climate	10
3. Power-Spectrum Method	24
4. Statistically Determined Features of African Waves	36
4.1 Statistical Significance of Spectral Results	36
4.2 Analysis of Time Series of Zonal and Meridional Wind	38
4.2.1 General Characteristics of Power Spectra of Horizontal Wind Components	38
4.2.2 The Source Region of African Waves	43
4.2.3 Vertical Structure of the Waves as Determined from the Meridional Wind	49
4.2.4 Vertical Influence of African Waves	51
4.2.5 Horizontal Wavelength of Waves	51
4.2.6 Horizontal Tilt of Wave Axis	55
4.2.7 Monthly Variations of Wave Activity	56
4.2.8 Seasonal Variations of Wave Amplitude	58
4.3 Analysis of Temperature, Specific Humidity and Geopotential Height	62
4.4 Horizontal Transports by African Waves	68
5. Discussions of Possible Causes of African Waves	74
5.1 Airflow over Mountains	74
5.2 Squall Line Formation over Elevated Land Areas	76
5.3 Barotropic Instability	77
5.4 Baroclinic Instability	81
6. Discussions and Conclusions	86
Acknowledgements	92
Appendix	93
Bibliography	97
Biographical Sketch	100

## Chapter 1

### Introduction

The most spectacular and most destructive meteorological phenomenon in low latitudes is the tropical hurricane. The complete devastation of property and great loss of human life which result from the most severe hurricanes have prompted considerable scientific effort toward finding a method for mitigating these devastating storms. Although the dynamics involved in the intensification of tropical storms are sufficiently understood so that the life cycle of a hurricane can be simulated numerically on high speed computers (see e.g. Ooyama, 1969), there is much that remains unknown about the development of hurricanes in the real world. For instance, while it is known that tropical cyclones generally intensify from pre-existing wavelike disturbances (Riehl, 1945), the origin of these disturbances remains a mystery. Over the ocean these disturbances are most frequently observed either along the Intertropical Convergence Zone (ITC) or completely within the easterly trades. While the waves in the ITC are thought to be produced by the horizontal shear instability of the converging trade winds in cooperation with cumulus convection (Bates, 1969), no adequate explanation has yet been given for the waves in the easterlies.

The most important achievement with regard to describing the basic characteristics of easterly waves<sup>1</sup> in the tropics has been the availability of daily satellite pictures of global extent. This was

---

<sup>1</sup>In the context of this paper the term easterly wave is intended to include any wavelike disturbance in tropical latitudes which propagates toward the west.

first accomplished on an operational basis during the late 1960's. Satellites are now providing daily information on vast tropical oceanic areas which had previously been void of any meteorological data. This has made it possible to coordinate reports from the widely separated regions of adequate conventional observations and to form a comprehensive description of synoptic-scale circulations in low latitudes.

In the central and eastern North Pacific satellite pictures reveal that the ITC is connected to most tropical disturbances (Denney, 1969); but because of the complete lack of conventional observations in this region, little is known about these disturbances. Only their most rudimentary characteristics have been determined from satellite information. In the corresponding part of the North Atlantic the majority of the perturbations are seen several hundred miles poleward of the ITC. From June to early October these Atlantic disturbances are recognizable on satellite pictures as "inverted v's" and cloud blobs (Frank, 1969). The "inverted v" is an oceanic manifestation of easterly waves which can be tracked back to central Africa by both satellites and conventional data; but near the Greenwich meridian the organized cloud pattern ceases to exist and at 20°E ground observations become very sparse with the result that it has been impossible to determine the precise origin of the disturbances (Carlson, 1969b).

Little progress has been made toward understanding the origin and dynamics of the African waves even though it was speculated prior to World War II that the African continent might be a source region for summertime disturbances in the Caribbean. Before the satellite era

the almost complete lack of observations over the Atlantic Ocean precluded regular tracking of disturbances across the ocean; nevertheless, Hubert (1939) succeeded in determining an African origin for the 1938 New England hurricane. Most observations of tropical disturbances in the western hemisphere were confined to the vicinity of the Caribbean where Dunn (1940) was the first to notice a westward progression of areas of rising and falling pressure at regular intervals of three or four days. Although most of these waves in the pressure field progressed through the Caribbean without significant change, those cyclones which intensified within the data network had been previously noted as disturbances in the surface pressures. Further study of these perturbations led to the easterly wave model which was first developed by Riehl (1945). He observed waves traveling through the Caribbean with an average wavelength of 2000 km and a cold core from the surface to 600 mb. These disturbances propagated toward the west at about 15 knots with upward motion and precipitation occurring to the east of the trough line. On the basis of their investigations in the Caribbean both Dunn and Riehl hypothesized that the easterly waves probably originated somewhere over the African continent.

Piersig (1936) was among the first to document cyclones which moved from western Africa into the eastern Atlantic. He used ship observations accumulated from 1881 to 1911 for his data and noted that these cyclones occurred during the same season as Atlantic hurricanes. Utilizing surface pressure data from land stations near the west coast of Africa, Regula (1936) observed westward propagating disturbances

with a period of four days and a wavelength of 2000 km: characteristics very similar to those described by Riehl for the Caribbean.

Disturbance lines which appear to be generated by late afternoon heating over north-south mountain ranges were investigated in southern West Africa by Hamilton and Archbold (1945) and Eldridge (1957). Although considerable confusion between the disturbance lines and easterly waves has persisted for many years, Schove (1946) recognized them as separate phenomena and concluded that the westward propagating trough lines rather than the squall lines are the predecessors of the waves observed in the Caribbean.

Prior to the first TIROS satellites investigations of easterly waves were conducted separately on either side of the Atlantic. Over the ocean the small amplitude of the waves at the surface and the absence of regular meteorological information made identification of the weak perturbations extremely difficult even after tropical cyclone intensity had been attained. Arnold (1966) extensively studied both the continent and ocean areas using conventional data from Africa and pictures from TIROS III following its launch in July of 1961. He concluded that there is a definite connection between disturbances over Africa and wave activity over the Atlantic Ocean. This finding is consistent with the climatology of easterly waves in the Atlantic recently compiled by Simpson et al. (1968, 1969) and Frank (1970) who have categorized all tropical Atlantic disturbances from 1967 to 1969. For these years it was found that the majority of disturbances reaching the Caribbean from the east during the summer can be traced to Africa

and comparatively few originate within the Atlantic ITC. Although only a small number of African waves ultimately intensify, these waves account for about half of the tropical Atlantic cyclones observed during August and September (Carlson, 1969b).

During 1967 and 1968 Carlson (1969a, 1969b) made daily synoptic analyses over tropical West Africa between the longitudes of  $20^{\circ}\text{E}$  and  $20^{\circ}\text{W}$ . Using surface, 2000-ft and 10,000-ft maps, he completed the first comprehensive examination of synoptic-scale disturbances over Africa and determined that there were many wavelike disturbances which formed east of the African bulge and propagated westward far to the south of the surface confluence zone (ITC) in the southern Sahara. These easterly waves reached a maximum amplitude near 600 mb in the lower tropospheric easterlies near  $10^{\circ}\text{W}$  and ultimately many progressed across the Atlantic Ocean. There was no detectable relation between the strength of an African wave and its subsequent development over the ocean. These waves were found to have a wavelength of 1300 nm and a period of about  $3\frac{1}{2}$  days. Although it appeared that some waves formed within the data network, many of the waves propagated into the analysis region from the east. The absence of a recognizable cloud pattern associated with the waves over eastern Africa and the lack of sufficient surface observations prevented the source region of the African waves from being clearly identified.

In spite of the vital role of African waves in the development of tropical storms in the Atlantic region, the climatology and kinematics of these waves have only recently been described and their origin



both in terms of location and dynamics has heretofore not been determined. The research presented in this thesis grew out of a desire to gain a better understanding of the origin of African waves. Power-spectrum techniques have been used to analyze time series of upper-air data at eight stations in North Africa. The statistics of westward propagating waves with a periodicity of 4-5 days<sup>1</sup> have been investigated and related to the monthly mean atmospheric circulation over Africa. The structure and source region of African waves are determined and the dynamics which relate to the generation of the waves are examined.

---

<sup>1</sup>African waves are a turbulent phenomena which produce an increase in the spectral density of the meridional wind at periods from three to almost six days. At 700 mb the spectral peaks generally occur at periods of 4.0 or 4.4 days. For convenience the waves are described as having a spectral peak at 4-5 days or a periodicity of 4-5 days.

## Chapter 2

### Description of the North African Summer Climate

Previous studies have speculated that African waves develop over the African continent. Since the presentation of statistical evidence supporting this hypothesis is a fundamental purpose of this thesis, it is appropriate to describe the properties of the African circulation for the months which overlap the African wave season.

For purposes of orientation a map of Africa (Fig. 2.1) is included in which the upper-air stations used in this study are identified and land elevations are indicated at intervals of one thousand meters. The North African summertime circulation from May to October is depicted by monthly averaged surface maps and meridional cross sections near 5 and 35°E (Figs. 2.2 to 2.7); the observing stations which were utilized in the cross sections are joined by dashed lines in Fig. 2.1. The surface temperatures, pressures and rainfall are ten-year averages from 1951 to 1960 which were plotted from World Weather Records (1968) and the gradient-level winds were reproduced from Atkinson and Sadler (1970). The information for the cross sections was obtained from data for the period from July 1957 to December 1964 which were processed by Professor R.E. Newell and students at MIT. These observations were supplemented with reports from Port Sudan and Malakal for the years 1964 to 1966 which were purchased from the National Climatic Center, Asheville, North Carolina.

The average latitude of the ITC over North Africa varies with season in response to solar heating and the climate of North Africa can

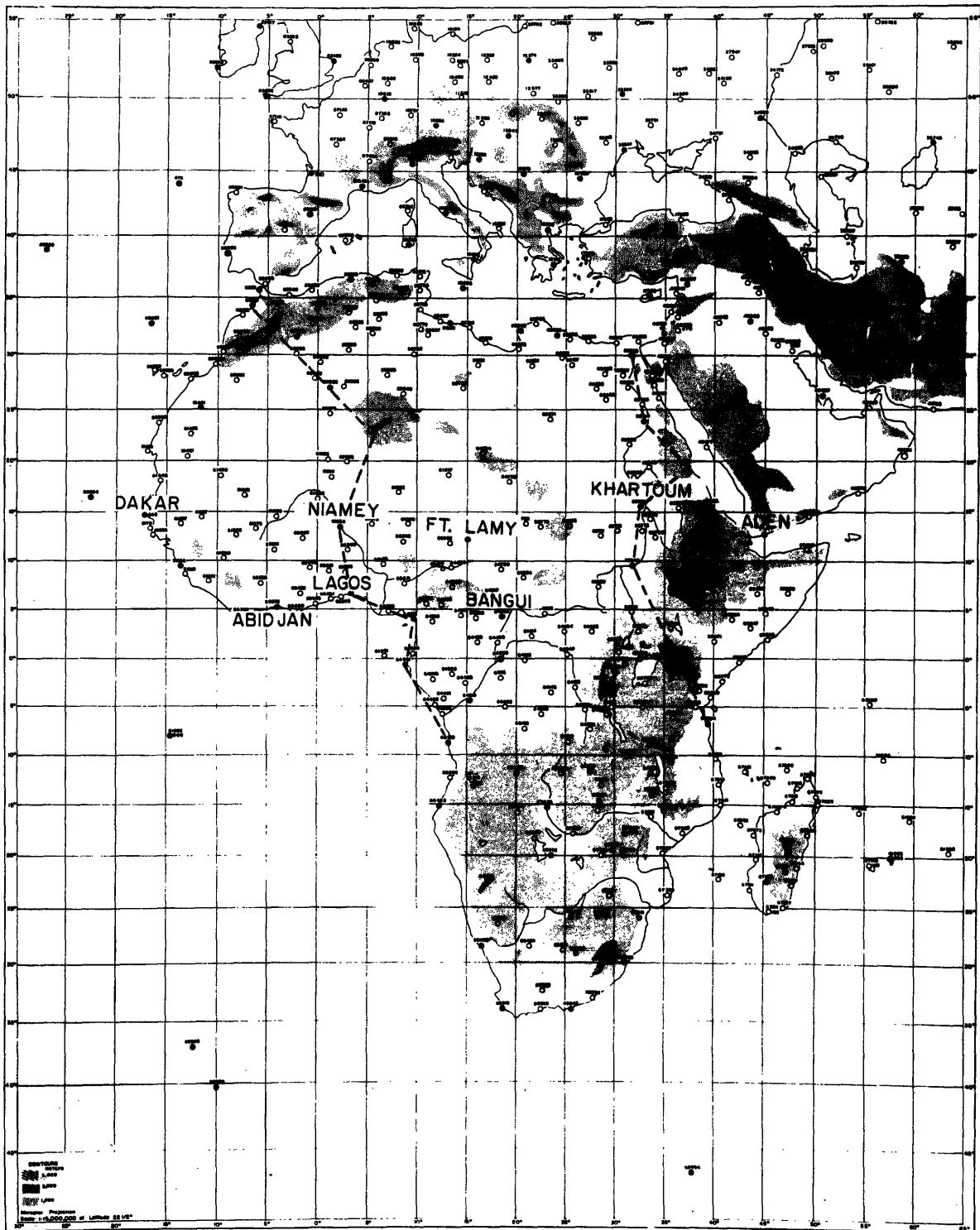


Fig. 2.1. Map of Africa with names and locations of upper-air stations used in the spectral analysis; the dashed lines join the stations used in the meridional cross sections.

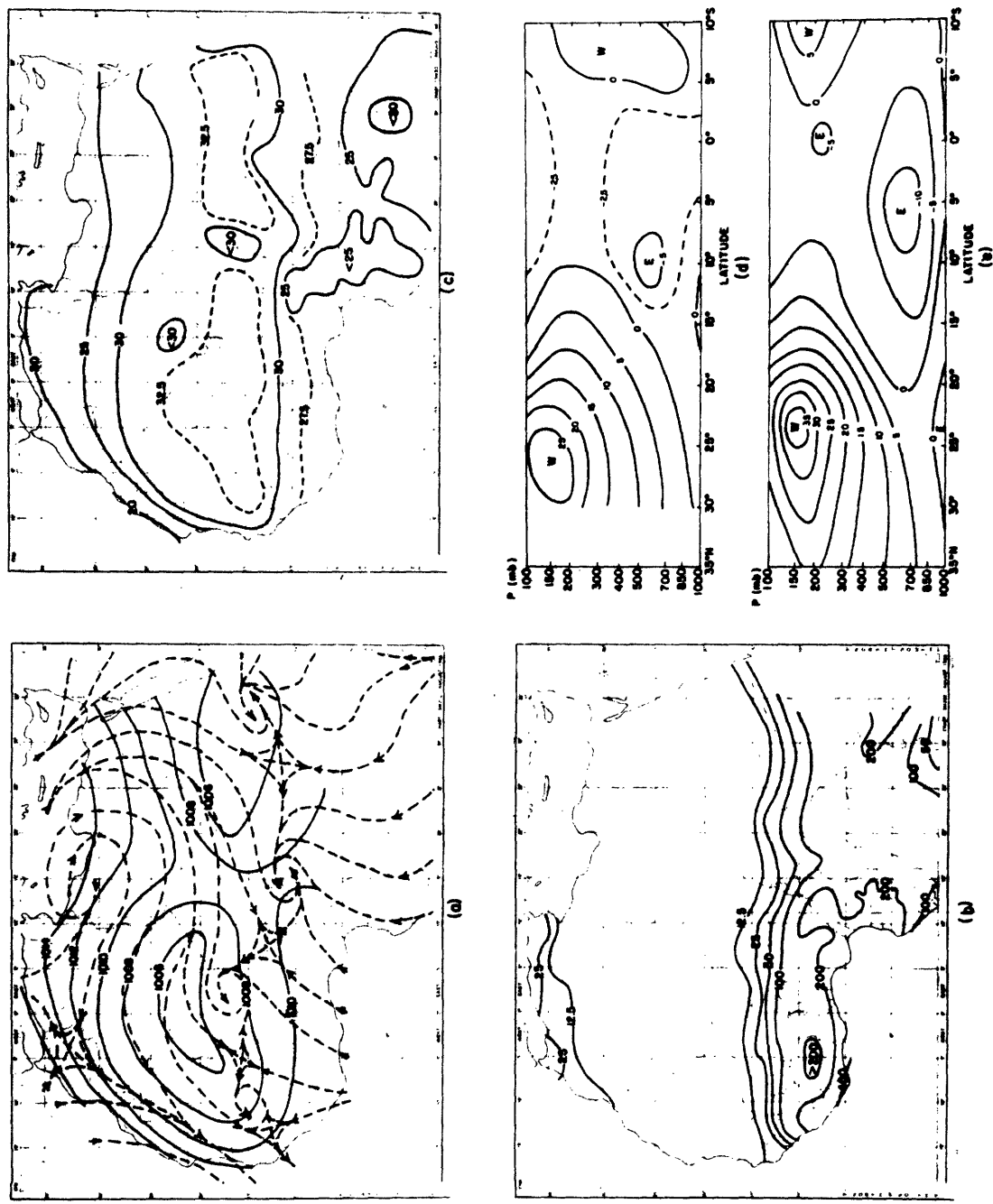


Fig. 2.2. Monthly mean maps for May, (a) surface pressure in mb and gradient-level wind, (b) daily average surface temperature in °C, and (c) daily average surface rainfall in mm, (d) and (e) meridional cross sections of zonal wind (m sec<sup>-1</sup>) at 35° and 5°E, respectively.

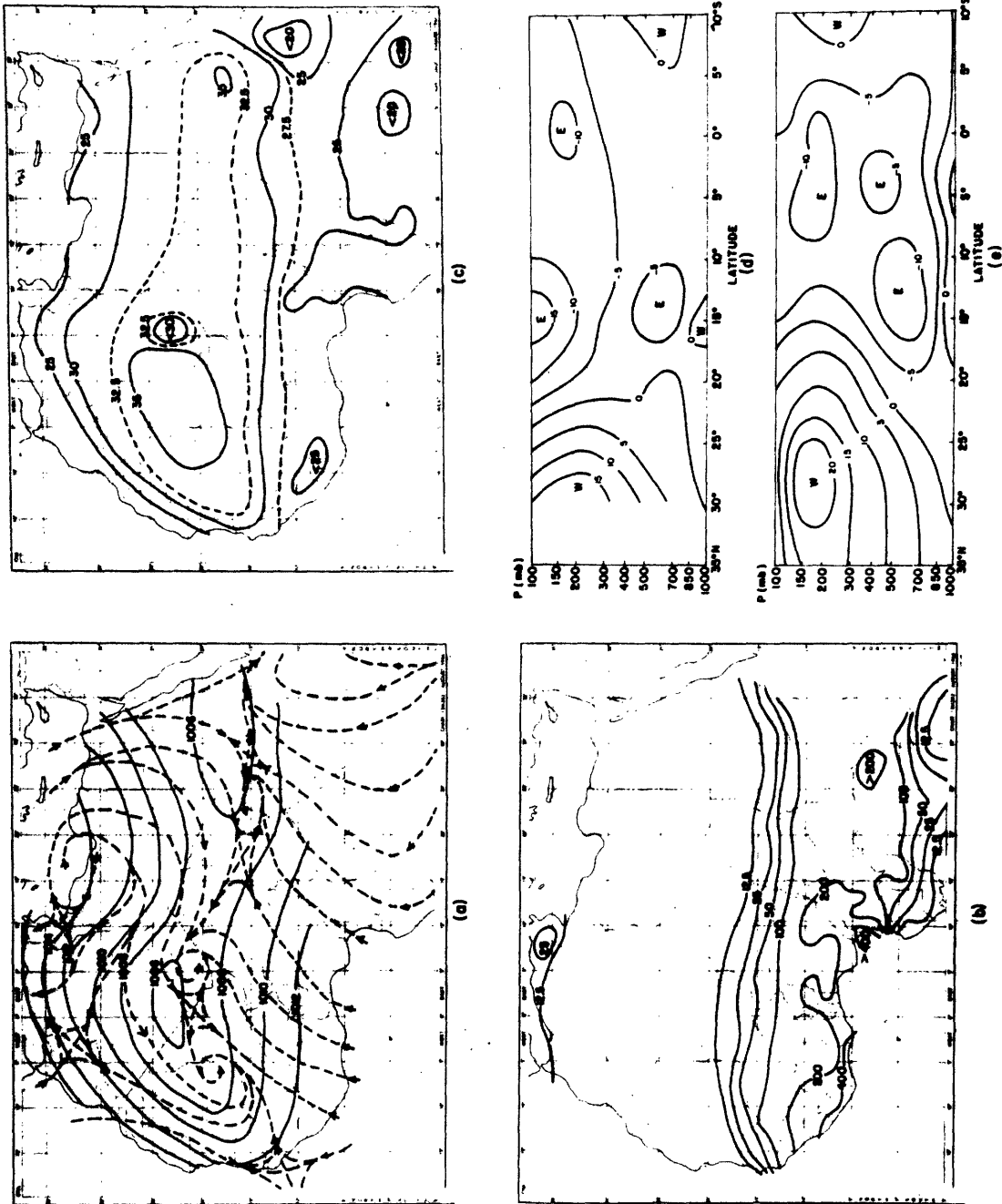


Fig. 2.3. Monthly mean maps for June; legend identical to Fig. 2.2.

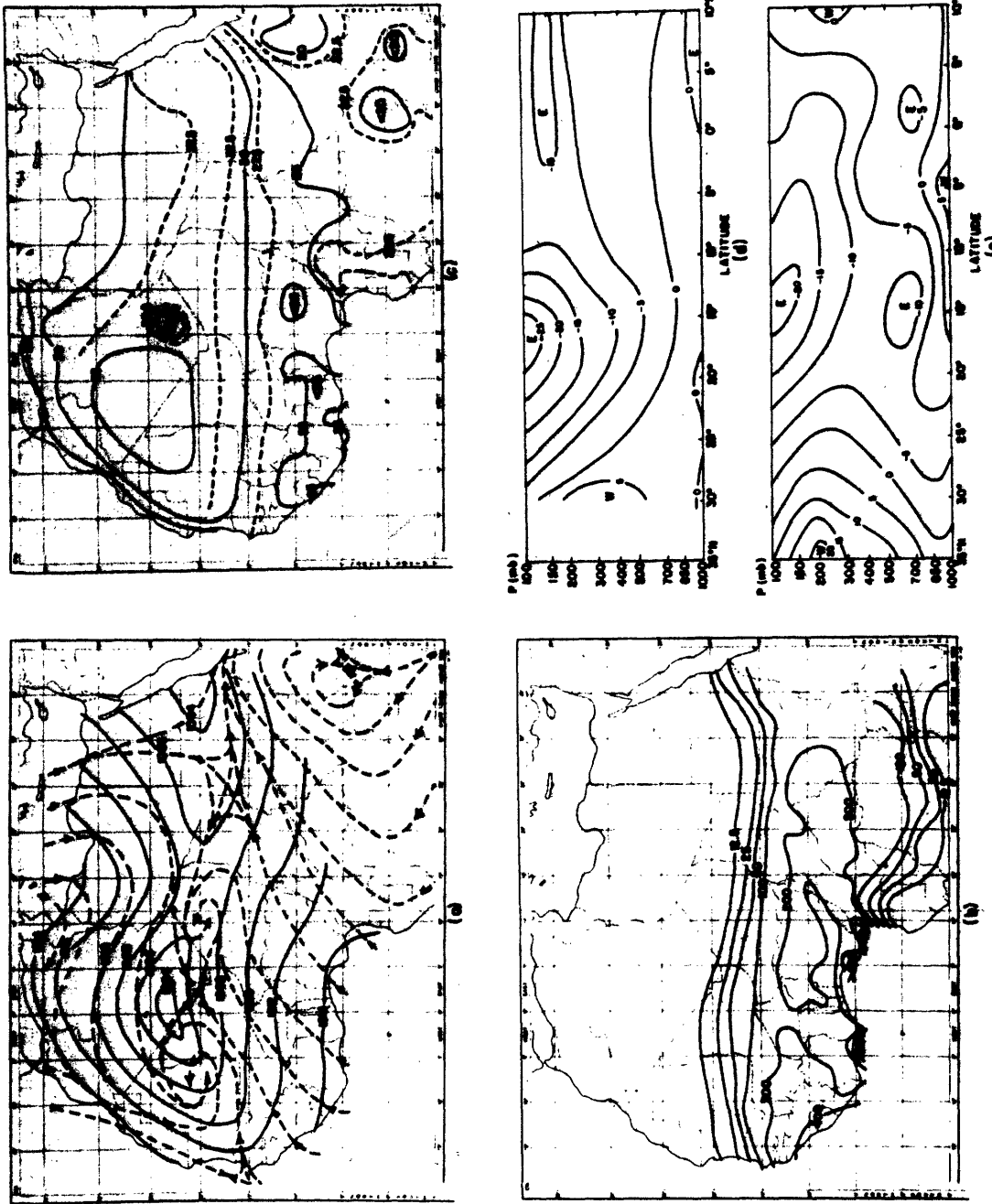


Fig. 2.4. Monthly mean maps for July; legend identical to Fig. 2.2.

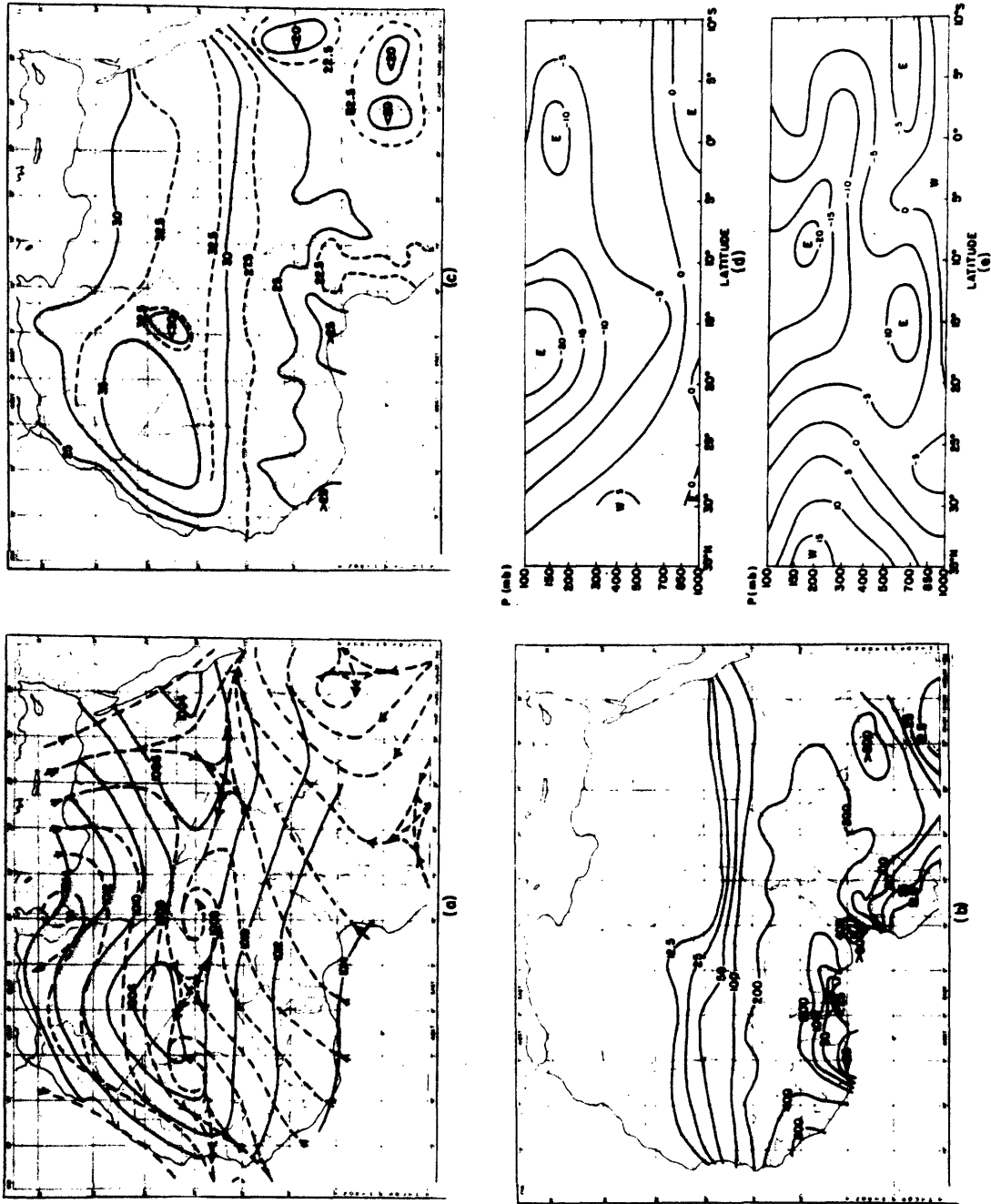


Fig. 2.5. Monthly mean maps for August; legend identical to Fig. 2.2.

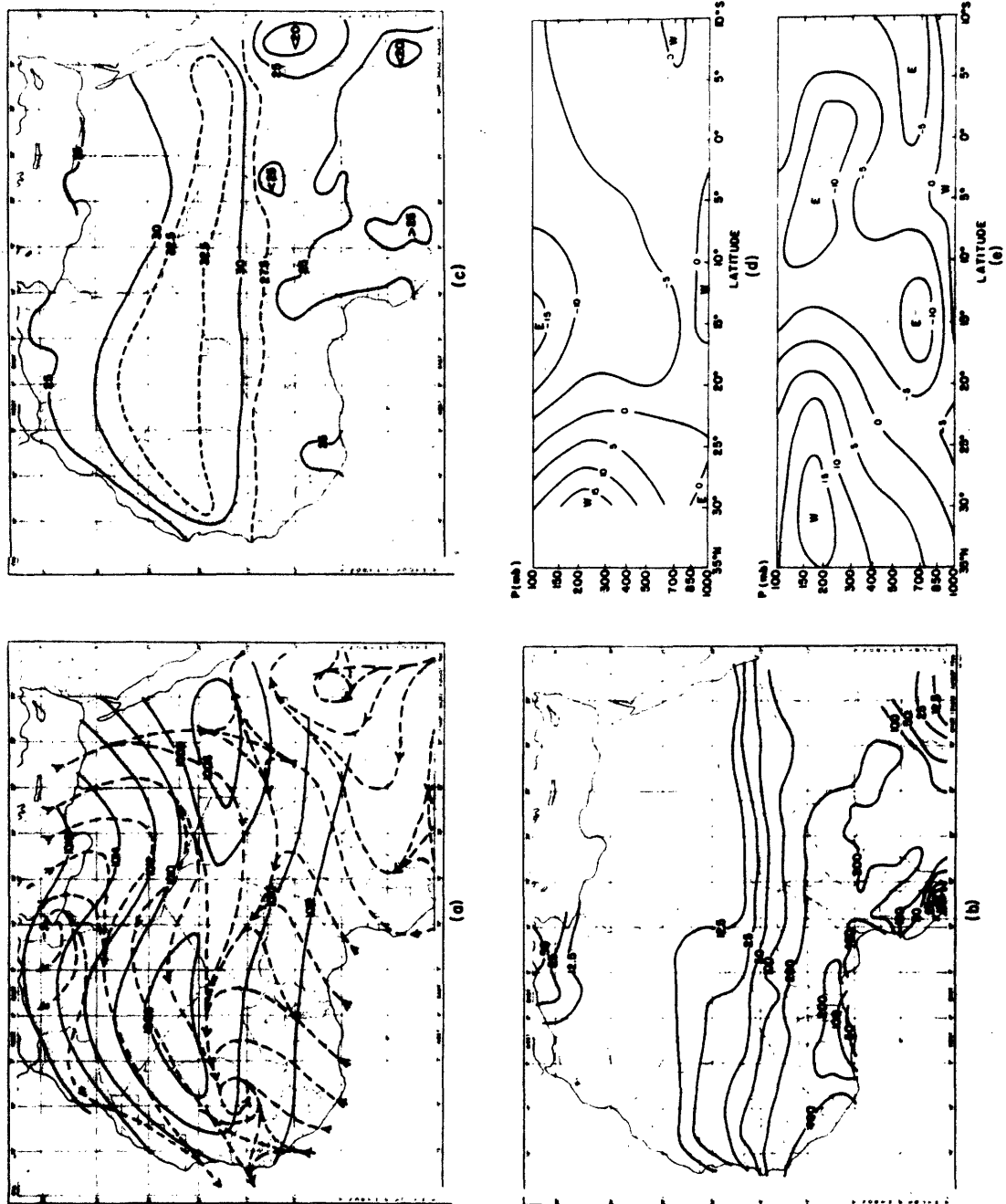


Fig. 2.6. Monthly mean maps for September; legend identical to Fig. 2.2.



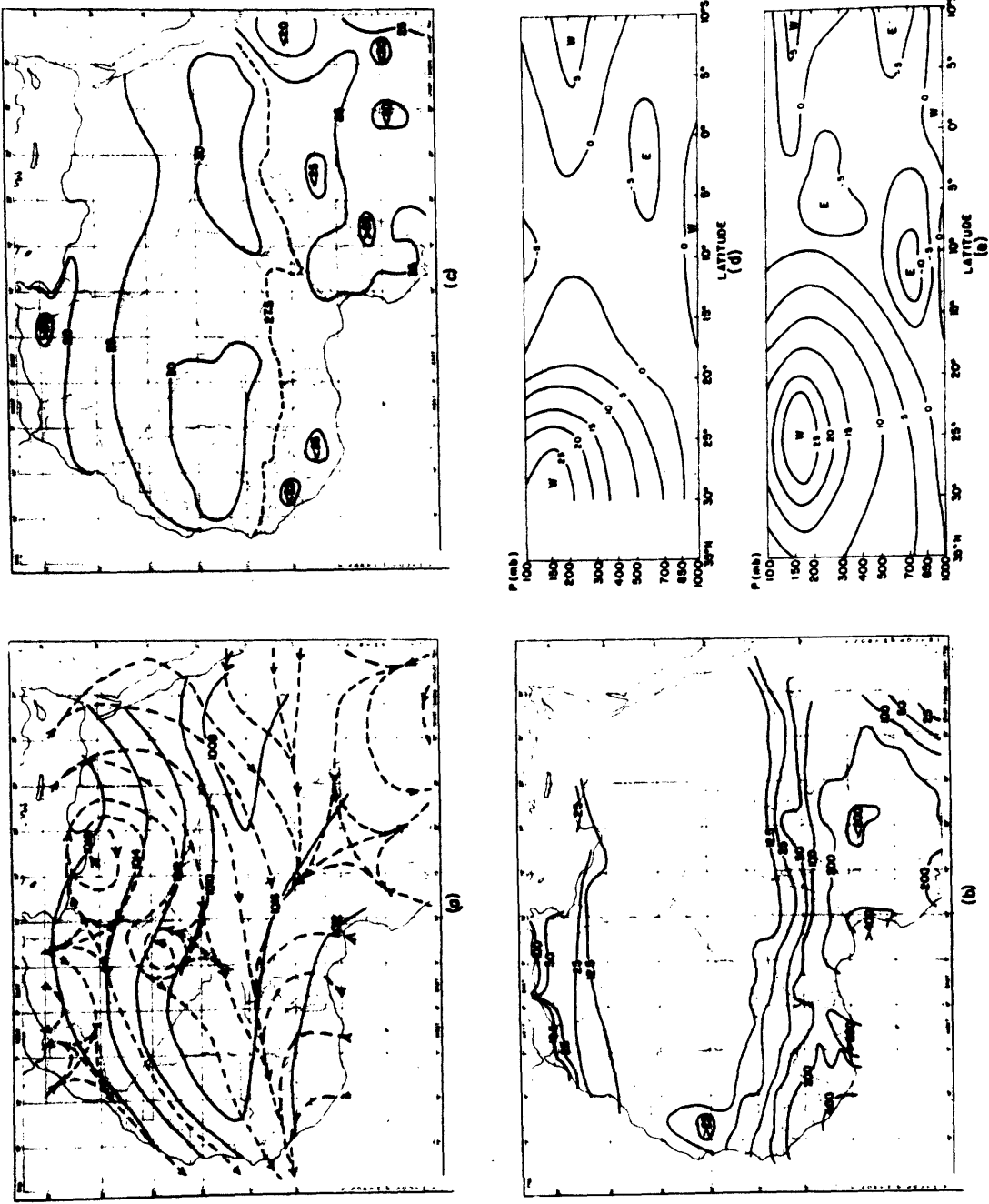


Fig. 2.7. Monthly mean maps for October; legend identical to Fig. 2.2.

be characterized generally by distinct zones which are fixed relative to the ITC. Within these zones prominent small-scale variations in mean rainfall and temperature are caused by local orographic and oceanic influences. Although these variations are important locally, they are ignored in this discussion of the meteorological features common to large areas of North Africa.

The maximum daily average surface temperature, which is usually found near and parallels the minimum surface pressure, is farthest south near  $7^{\circ}\text{N}$  during January and February and most poleward north of  $20^{\circ}\text{N}$  during July and August. Over the North African land mass the ITC coincides with the minimum surface pressure; it is essentially a thermal low which is elongated in the east-west direction. Consequently the weather in its vicinity differs considerably from that associated with oceanic portions of the ITC. Although the North African ITC is a zone of strong confluence, little or no rain falls in its vicinity because of the extreme dryness of the surface air on its poleward side and mean tropospheric subsidence aloft (see e.g. Kyle, 1970). At the ground the ITC marks the discontinuity between the cool, moist maritime air of the southwest monsoon of West and Central Africa and the warm, dry desert air from the Sahara to the north.

Surface temperatures reach a maximum over Central Africa during July and August but change very little from season to season near  $5^{\circ}\text{N}$  over West Africa due to the moderating influence of the Atlantic Ocean. The surface temperature gradient, therefore, is strongest during the summer months. In the middle troposphere the meridional cross sections

show that the temperature is nearly uniform from the equator to  $25^{\circ}\text{N}$ . On the other hand a latitudinal cross section of monthly mean zonal winds for those stations near  $10\text{-}15^{\circ}\text{N}$  reveals that there is westerly shear of the zonal wind from 600 to 400 mb (Fig. 2.8). The westerly shear indicates by means of the thermal wind equation that warm air is equatorward and cool air poleward of this region. The observed wind shear is not consistent with the temperature field; however, the wind field is considered to be more accurate and the temperature field implied by the shear of the zonal wind is felt to be representative of the actual temperatures.

As a response to the surface baroclinic zone and the reversal of the temperature gradient in the middle troposphere, there is an east-wind maximum near 600 mb which is strongest and farthest poleward in July and August. This mid-tropospheric east-wind maximum is present during the entire year above the baroclinic zone. Although easterly flow is relatively weak on the  $35^{\circ}\text{E}$  cross section, the current becomes organized into a well defined jet over the western two-thirds of Africa from April to November. This phenomenon is distinctly separate from the easterly wind maximum near 150 mb which is a remnant of the Indian monsoon jet found to the south of the Tibetan anticyclone from June through September.

Hamilton and Archbold (1945) described the climate of North Africa in terms of latitudinal zones which are fixed relative to the surface ITC. These same zones (see Fig. 2.9 for August) are appropriate for this discussion but are additionally interpreted with regard to

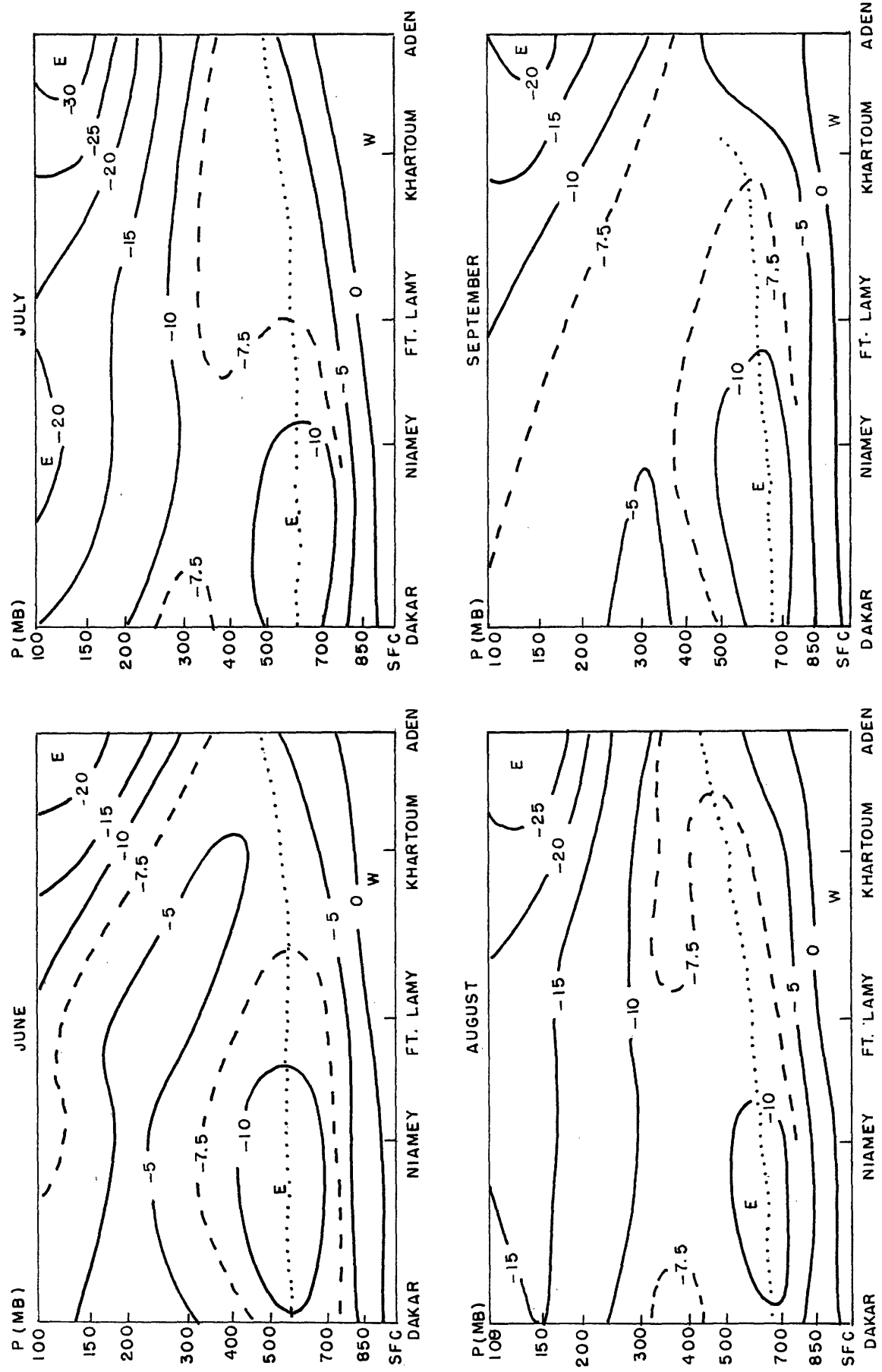


Fig. 2.8. Cross section of monthly mean zonal wind ( $m\ sec^{-1}$ ) along  $13^{\circ}N$ ; dotted line indicates the position of the easterly wind maximum in the middle troposphere.

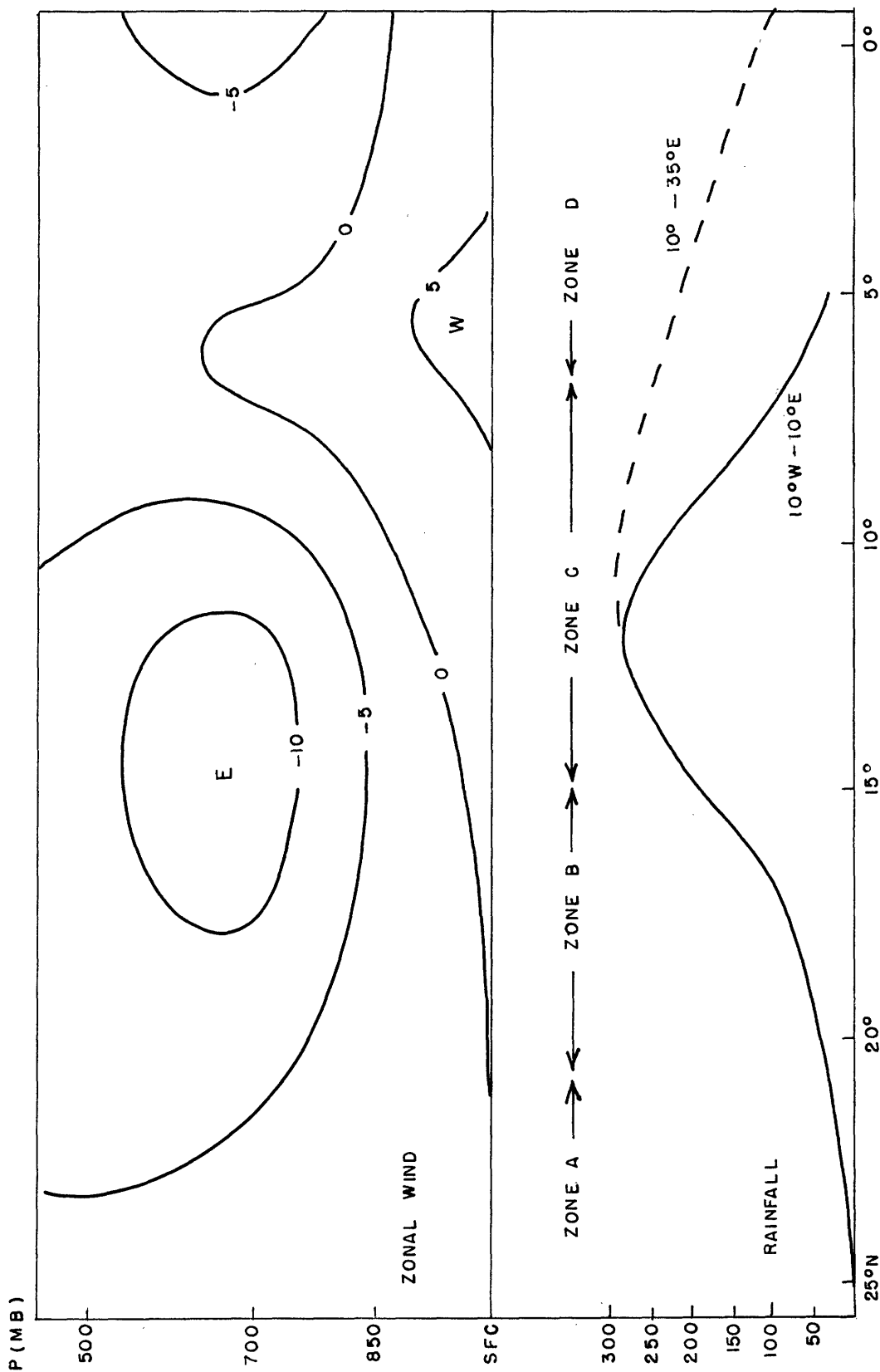


Fig. 2.9. Idealized meridional cross section near 5°E for August; winds are in  $m\ sec^{-1}$  and rainfall in mm.

the upper-air observations processed during this study. The description of these zones is generally valid during the African wave season from 35°E to the Atlantic Ocean except that zone D exists only between 10°W and 10°E.

Zone A lies poleward of the surface ITC in very arid, desert regions of the continent. The air throughout the troposphere is extremely dry and the skies are generally cloudless although frequently dusty and hazy. The combination of dry air and low heat capacity of the ground produces a large diurnal variation of surface temperature (approximately 25°C). There is a strong inversion near the ground at night, but during the time of maximum daytime heating the lapse rate is nearly dry adiabatic up to 500 mb and vigorous deep but dry convection results. Near the 500-mb level there is frequently an inversion which is apparently caused by warming from mean subsidence in the middle troposphere (Kyle) above the layer of dry convection.

Zone B is the region immediately equatorward of the ITC in the baroclinic zone at the surface and on the anticyclonic shear side of the easterly jet. In this area cloud bases are quite high and thunderstorm activity is infrequent. Monthly mean precipitation is light (on the order of one inch) and is inhibited by the extremely dry air above the moist surface southwesterlies which are no more than 1000-2000 ft thick.

Zone C lies in the southern part of the surface baroclinic zone and on the cyclonic shear side of the easterly jet. This is a region of maximum rainfall in which squall lines are frequent and African wave

activity is centered. The amount of precipitation increases as the depth of the southwesterlies increases and thunderstorms are common. Much of the precipitation is associated with the passage of squall lines (Eldridge, 1957) which are sometimes referred to as West African tornadoes.

Zone D represents the south coastal region of the African bulge during July, August and September except where orographic upslope motion fantastically increases the monthly average precipitation. Although the surface air is extremely moist, there is an inversion near 800 mb which suppresses deep convection. During the summer months of the year sea-surface temperatures in the Gulf of Guinea reach a minimum (U.S. Navy, 1955); the air traversing the Gulf of Guinea is cooled during its over-water trajectory with the result that convection is generally unable to penetrate the stable layer near 800 mb. In the absence of any mechanism for forced ascent there is a persistent layer of thin stratus. Precipitation may occur but monthly rainfall totals are generally less than an inch.

A major difference between the North African circulation and normal tropical oceanic or middle-latitude weather patterns is that warm advection and moisture advection are highly negatively correlated in North Africa. The warm desert air is dry and the moist maritime air is cool. This considerably complicates the synoptic patterns of precipitation since, for instance, the advection of warm but extremely dry air will not likely lead to saturation.

## Chapter 3

### Power-Spectrum Method

African waves have been investigated synoptically since the mid 1960's, but the physical processes responsible for the generation of these disturbances are not clearly understood because their source region has not yet been identified. While the seasonal characteristics, mean wavelength, mean period and rate of propagation of African waves have been described by Carlson (1969a, 1969b), further study of constant-level maps with the existing observing network probably will not contribute significantly to present knowledge. Recently Yanai et al. (1968) and Wallace and Chang (1969), among others, have shown that spectrum analysis is a very powerful method for obtaining information on the basic statistical properties of zonally propagating disturbances in the troposphere. This method has been particularly informative in regions where the observing stations are too widely separated for conventional synoptic techniques. Since the upper-air observing network over Africa is also very sparse, spectrum analysis offers a meaningful approach for more extensive investigation of African waves with the current density of stations.

The upper-air data used in this study were obtained on cards from the National Climatic Center in Asheville, North Carolina, for the eight stations listed in table 3.1. These were the only stations in the latitudinal zone of African wave activity which took observations often enough for spectral analysis of waves whose period is



Table 3.1

<u>Station</u>	<u>Latitude</u>	<u>Longitude</u>	<u>WMO No.</u>	<u>Hour of Observation</u>	<u>Elevation Meters</u>
Abidjan	5° 15' N	3° 56' W	65578	06Z(00Z in 1964)	7
Aden	12° 50' N	45° 2' E	40597	00Z	3
Bangui	4° 23' N	18° 34' E	64650	06Z(00Z in 1964)	366
Dakar	14° 44' N	17° 30' W	61641	12Z(00Z in 1961)	24
Ft. Lamy	12° 8' N	15° 2' E	64700	06Z(00Z in 1964)	295
Khartoum	15° 36' N	32° 33' E	62721	06Z	380
Lagos	6° 35' N	3° 20' E	65201	06Z(12Z in 1964)	38
Niamey	13° 29' N	2° 10' E	61052	06Z(00Z in 1964)	234

In several tables in chapter 4 the stations are grouped from east to west in the following manner

Aden	}	approximately 13° N
Khartoum		
Ft. Lamy		
Niamey		
Dakar		

Bangui	}	approximately 5° N
Lagos		
Abidjan		

approximately four days. The number of soundings taken at each station was tabulated and the years 1960 to 1964 were selected for study because observations were more frequent during these years. It was somewhat arbitrarily decided that a five-year record would be adequate for obtaining meaningful statistical results. The months from May to November were selected for examination because these months overlap the period from mid June to early October when African waves are generally observed. Each station reported once per day and Lagos in particular had a large number of missing observations but no attempt was made to interpolate for missing data. Fort Lamy and Bangui took measurements of temperature and dew point for just one year, therefore, only wind observations were analyzed for these stations. Time series of zonal and meridional wind, temperature, specific humidity and geopotential height were formed at the nine available mandatory levels from the surface to 100 mb excluding 1000 mb. In order to eliminate grossly erroneous reports, all observations more than three standard deviations from the sample mean were rejected. Presumably a small fraction of valid observations were rejected by this method but this was tolerable in view of the fact that the data had not been checked previously for errors.

Since power-spectrum and cross-spectrum methods are designed to isolate periodic components, it is of utmost importance to choose data samples which are nearly stationary with respect to the phenomenon being investigated. In an attempt to limit the data to a time during which African wave activity was stationary, two different sampling

periods were used in creating the time series for this study. The first sampling period, which is referred to in the text as seasonal time series, included the time from July 15 to September 30 when African waves propagate most uniformly and the second treated each month separately (monthly time series). Frank (1970) has indicated that there was very little difference between the total number of African waves in 1968 and 1969 even though the Atlantic tropical cyclone season was considerably more active during 1969. Since there was no other evidence available which suggested that there have been large year-to-year variations in the number of African waves, it was decided to treat the entire five years of data as a single sample. This has the advantage of greatly increasing confidence in the final results. An aposteriori examination of the results showed that this approach was justified.

Power spectra and cross spectra of the time series were computed by means of the covariance method which has been described by Bendat and Piersol (1966) and is discussed briefly in the appendix. A five-year average linear trend which was determined by least-squares fit was removed from each time series before analysis, but no other form of filtering was utilized. The five-year average trend was formed by averaging the linear trend calculated for each individual year. Extensive testing showed that the removal of the linear trend did not contribute to a false amplitude peak near the observed frequency of African waves and had generally negligible effects except at the very low-frequency end of the spectrum. The covariance curves were computed

with a lag of 20 days for the seasonal series and with a lag of 12 days for the monthly series; the five-year average covariance curve was formed by averaging the covariance curves for each year.

A fundamental problem for studies involving statistical results is the choice of criteria by which definitive statements may be either accepted or rejected. Since an important goal of this study is the isolation of the source region of African waves between adjacent stations, a method is needed for determining the existence or non-existence of a significant peak in the power spectrum at periods corresponding to these waves. Since no generally accepted method was available, an adequate test had to be developed. Initial research with the data at Dakar indicated that the passage of African waves produced an increase in variance over a broad range of periods from three to five and one-half days. The main objective, therefore, was to determine the maximum, mean and minimum amount of variance which would be expected in this range of periods on the basis of chance. In order to ascertain the magnitude of chance variations in the power spectra, computations were made with series created by a random number generator. The mean one-day lag autocorrelation and the distribution about the sample mean were determined for the wind components at all levels for each station so that the random number series could match the actual data samples in these respects.

The random numbers were obtained from RANDU, an IBM 360 machine-specific subroutine (contained in the IBM Scientific Subroutine Package), which computes uniformly distributed random real numbers between 0.0 and

1.0. Seven successive numbers from RANDU were averaged in order to produce a new series with distribution properties about the sample mean which resembled that of the actual data. The randomly generated series were computed in the following manner

$$a_k = \text{random number from RANDU}$$

$$\text{define } b_j \equiv \frac{1}{7} \sum_{k=1}^{j+6} a_k$$

Then a new series  $\{c\}$  was defined in terms of  $p$  where

$$p = \text{lag-one autocorrelation value or "persistence"}$$

$$c_1 = b_1$$

$$c_j = p c_{j-1} + b_j \quad \text{for } j > 1$$

$c_1, c_2, \dots, c_{10}$  were used only as a means of starting the desired sequence of numbers  $c_{11}, c_{12}, \dots, c_{\text{LAST}}$ . The series  $\{c\}$  were spectrally analyzed in a manner identical to that applied to the real time series and experiments were conducted which simulated both the seasonal and monthly series. In order to approximate the observed range of lag-one autocorrelation values, tests were made with several values of  $p$  which varied from -0.25 to 0.50 in increments of 0.05. Thirty series of  $\{c\}$  were analyzed for each value of  $p$ . Because of the finite length of the random number series, the actual lag-one autocorrelation values of  $\{c\}$  deviate from the imposed value of  $p$  but generally by less than  $\pm 0.05$ .

Three sets of numbers were spectrally analyzed for each of these series: the first with no linear trend removed (method 1), the second with a linear trend removed (method 2) and the third with the linear trend subtracted and a periodic component added (method 3). Comparison of the results of method 1 and method 2 verified that the two procedures produced identical results except at the two or three lowest frequencies<sup>1</sup>. The power spectral density estimates for three series obtained with method 2 and  $\rho = 0.0$  (i.e. white noise) are shown in Fig. 3.1. This figure depicts chance fluctuations which occur in any given finite sample. Care must be taken to insure that variations similar to these are not considered to be significant. Fig. 3.2 reveals the effects of adding persistence (redness) and a periodic component which contains only ten per cent of the total variance but which is clearly isolated by the spectral procedure. Since persistence is a measure of power in the low-frequency components, the general shape of the spectral density function varies with  $\rho$ . It is readily apparent that the one-day lag autocorrelation must be considered when interpreting the statistical results.

At those stations known to be influenced by African waves, preliminary analysis revealed an increase of variance in the periods from three to five and one-half days. A satisfactory indicator of wave activity was found to be the per cent of the total variance (%TV) computed for the periods from 3.1 to 5.7 days for the seasonal

---

<sup>1</sup>The random number analysis was completed after the results with the actual data had been obtained and indicates that the removal of the linear trend was an unnecessary step.

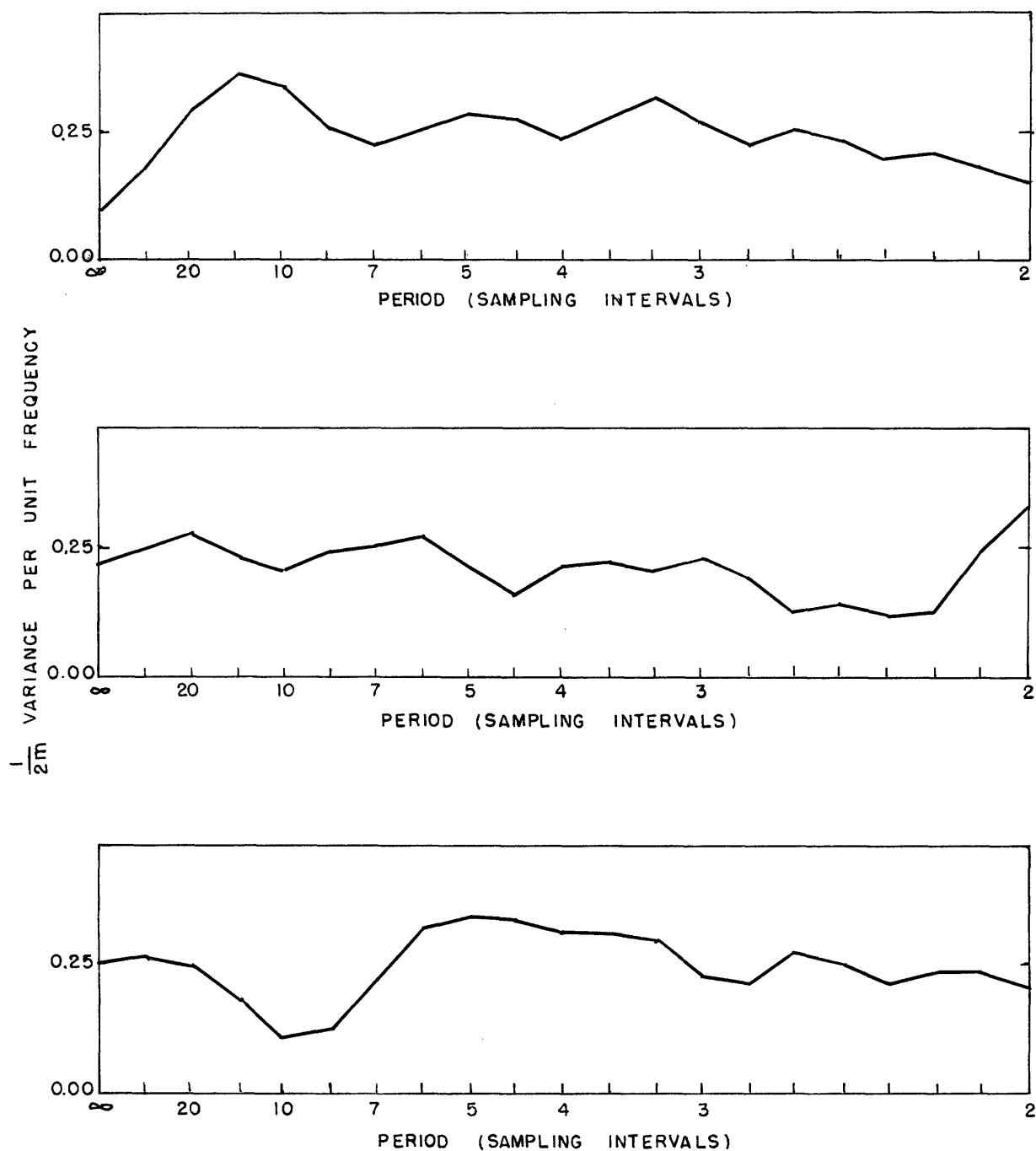


Fig. 3.1. Power spectral density estimates of three random number series which simulate the seasonal series with  $\rho = 0.0$  (white noise).

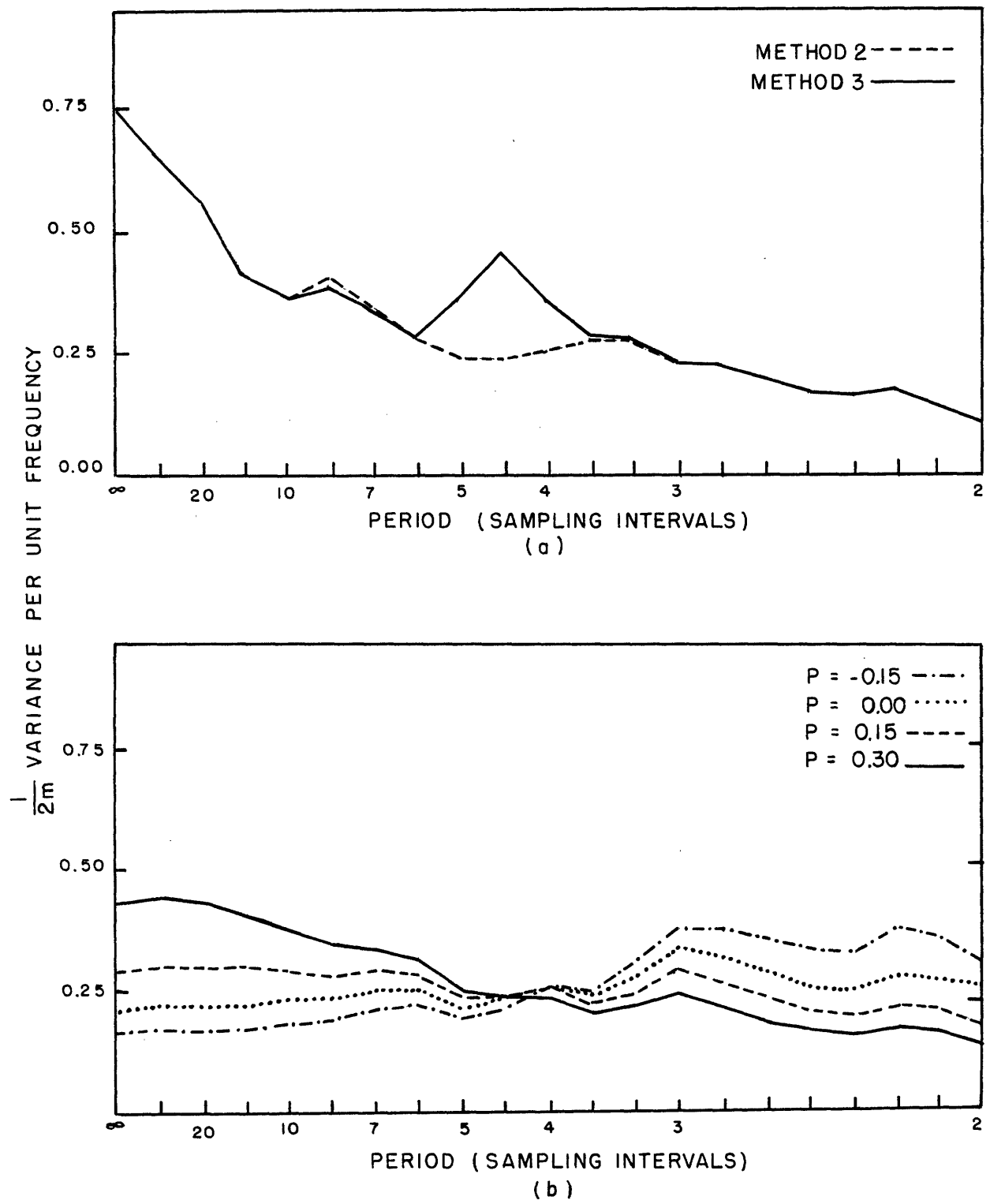


Fig. 3.2. Power spectra of random numbers which simulate the seasonal series, (a) sample series ( $\rho = 0.30$ ) with and without periodic component which contains ten percent of total variance, (b) single random number series but with four different values of  $\rho$ .



series and for the periods from 3.0 to 6.0 days for the monthly series. The %TV was calculated for each randomly generated series and a summary of these results is presented in tables 3.2 and 3.3. The value of %TV is normally distributed only for time series of pure white noise, however, the distribution of %TV in those series with some redness is undoubtedly sufficiently close to normal that variations from the mean of more than two standard deviations are significant.

There are two main reasons why the values in tables 3.2 and 3.3 represent approximate criteria for judging statistical significance. First, only thirty random number series have been used to obtain the statistics of %TV for each value of  $p$ . If an infinite number of series had been used, the value of %TV for  $p = 0.0$  for the seasonal and monthly series would be 35.0 and 41.7% respectively rather than the tabulated values of 34.2 and 42.0%. Second, there are missing observations in every time series so that the degrees of freedom in the calculations with the actual data are less than that for the random number series; therefore, the appropriate standard deviation of %TV for the observed data should be larger than that which is given in the tables. For these reasons African waves are assumed to exist at those levels and stations where the %TV deviates from the expected normal by more than two standard deviations and where there is a clear indication of a zonally propagating disturbance.

Table 3.2

Summary of calculations with random number series

Simulation of seasonal time series by method 2.

<u>P</u>	<u>30 Sample Average %TV</u>	<u>30 Sample Maximum %TV</u>	<u>30 Sample Minimum %TV</u>	<u>Standard Deviation of %TV</u>
-0.15	32.9	40.9	26.4	3.30
-0.10	33.6	41.3	27.6	3.34
-0.05	34.0	41.5	28.3	3.25
0.00	34.2	41.4	28.6	3.30
0.05	34.0	41.1	28.3	3.30
0.10	33.6	40.7	27.6	3.33
0.15	33.0	40.3	26.6	3.36
0.20	32.1	39.6	25.4	3.42
0.25	30.9	38.7	24.1	3.43
0.30	29.6	37.5	22.5	3.47
0.35	28.0	36.1	20.8	3.46
0.40	26.2	34.4	19.0	3.43
0.45	24.2	32.5	17.1	3.38
0.50	22.2	30.5	15.2	3.30

Table 3.3

Summary of calculations with random number series  
Simulation of monthly time series by method 2.

<u>p</u>	<u>30 Sample Average %TV</u>	<u>30 Sample Maximum %TV</u>	<u>30 Sample Minimum %TV</u>	<u>Standard Deviation of %TV</u>
-0.25	38.1	47.3	27.4	4.99
-0.20	39.4	49.1	29.0	4.99
-0.15	40.5	50.4	30.4	4.87
-0.10	41.3	51.4	31.8	4.85
-0.05	41.8	52.1	32.8	4.86
0.00	42.0	52.4	33.4	4.86
0.05	42.0	52.5	33.4	4.89
0.10	41.6	52.2	33.1	4.93
0.15	41.0	51.8	32.1	5.00
0.20	40.2	51.2	31.1	5.03
0.25	39.0	50.4	29.8	5.12
0.30	37.6	49.3	28.3	5.22
0.35	35.9	47.9	26.6	5.30
0.40	34.0	46.2	24.7	5.35
0.45	32.0	44.2	22.7	5.31
0.50	29.7	41.8	20.5	5.30

## Chapter 4

## Statistically Determined Features of African Waves

4.1 Statistical Significance of Spectral Results

Time series of zonal (u) and meridional (v) wind, temperature (T), specific humidity (q), geopotential height (z) and surface pressure ( $p_{sfc}$ ) were formed at the mandatory levels from the surface to 100 mb for each station listed in table 3.1. No attempt was made to analyze time series at 1000 mb since the normal surface pressure is lower than this at four of the stations.

The coherence (see appendix for details of computation) is an important quantity in cross-spectrum analysis which varies as a function of frequency. It is similar to the square of a correlation coefficient except that it measures out-of-phase correlation as well as in-phase correlation. The statistical significance of the coherence is a function of the number of degrees of freedom, which is the number of independent observations that contribute to each spectral density estimate. The number of degrees of freedom is defined by

$$\text{degrees of freedom} = \frac{2N}{m} - \frac{1}{2}$$

where N is the total number of data points in the time series and m is the number of lags. Since a few observations are missing in most of the time series, the individual spectral density estimates have 35 degrees of freedom for the seasonal time series and 23 degrees of freedom for the monthly time series. Phase difference and coherence in

several of the figures represent averages from 3.1 to 5.7 days and 3.0 to 6.0 days for the seasonal and monthly series respectively. These quantities were obtained by averaging individual co-spectral and quadrature spectral estimates within the range of periods rather than directly averaging the phase difference and coherence. When the number of missing observations, the use of the Hanning smoothing procedure and the averaging over several periods are considered, the averaged coherence has 125 degrees of freedom for the seasonal series and 60 degrees of freedom for the monthly series. Goodman has derived an approximate formula (see Panofsky and Brier, 1958, p. 158) for determining the minimum coherence value which represents a relationship between time series at the 95% significance level. This formula gives

Series	Period range in days	Degrees of freedom	Significant coherence at 95% level
monthly	3.0-6.0	60	.22
seasonal	3.1-5.7	125	.15

In each of the figures the units of the spectral density estimates are variance day. They can be converted to units of amplitude with the following relationship

$m$  = total lag number in days

$\bar{G}(\frac{kf_c}{m})$  = spectral density estimate  $k = 0, 1, \dots, m$

$$\text{amplitude} = \sqrt{\frac{\bar{G}(\frac{kf_c}{m})}{m}}$$

The symbol %TV is used frequently in the text, it is defined as the per cent of the total variance in the period range from 3.1 to 5.7 days for the seasonal series. The same symbol is also used for the monthly series but the per cent of the total variance is computed for the period range from 3.0 to 6.0 days.

## 4.2 Analysis of Time Series of Zonal and Meridional Winds

### 4.2.1 General Characteristics of Power Spectra of Horizontal Wind Components

Power spectral density estimates of the seasonal series of zonal and meridional winds were computed at each level for every station and are shown in Figs. 4.1 to 4.4 as a function of height and period. There are two features which are common to many of the spectra. The first is the spectral peak in the v component at periods near 4-5 days which reaches a maximum amplitude of 1-2 m/sec in the lower troposphere at 700 mb at all stations except Aden. This lower tropospheric spectral peak is usually not found above 400 mb but does tend to affect a deeper layer of the atmosphere toward the west coast of Africa. At 700 mb the periods from 3.1 to 5.7 days account for approximately fifty per cent of the total variance of the v component but no corresponding peak in the u spectrum is observed. The amplitude of the u power spectral density estimates is smaller than those for v near 4-5 days so that the kinetic energy is mainly confined to the meridional wind. In general the zonal wind contains much more energy at the low-frequency end of the spectrum than the meridional wind. The second consistent feature at many of the stations is the concentration of variance near

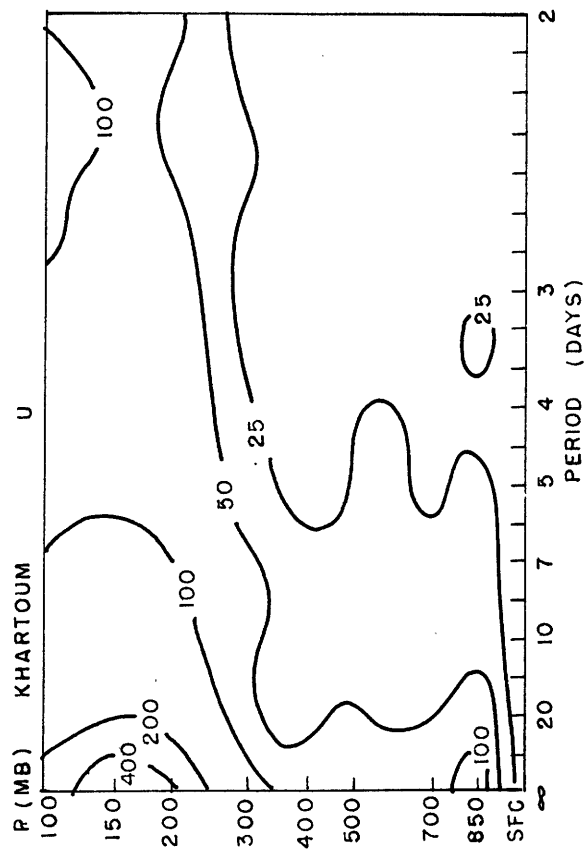
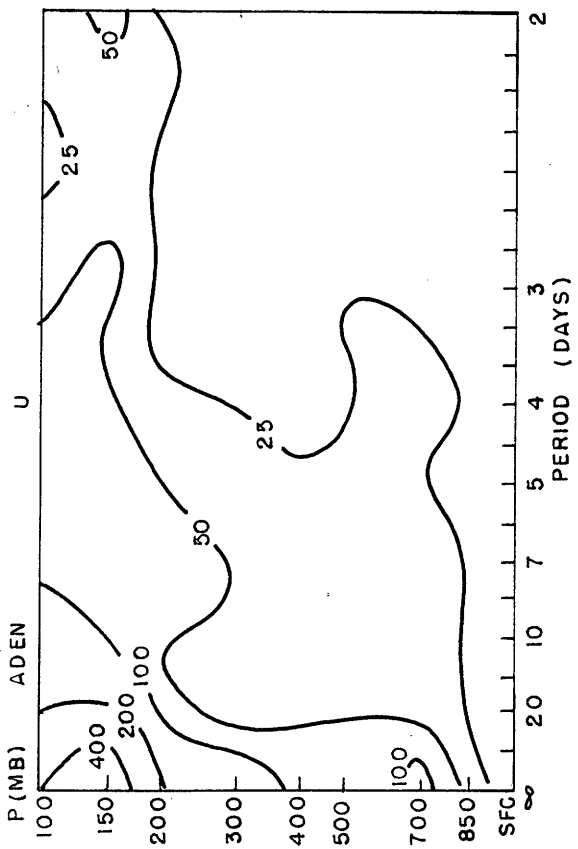
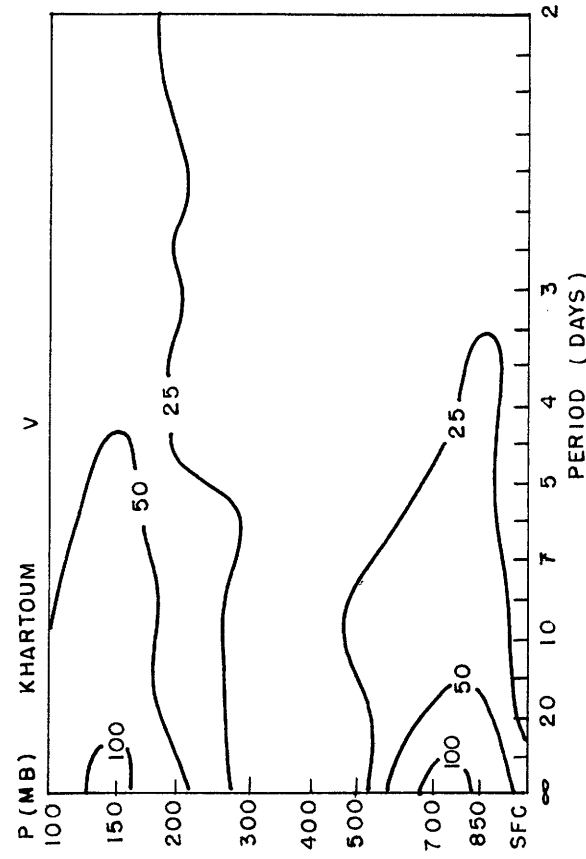
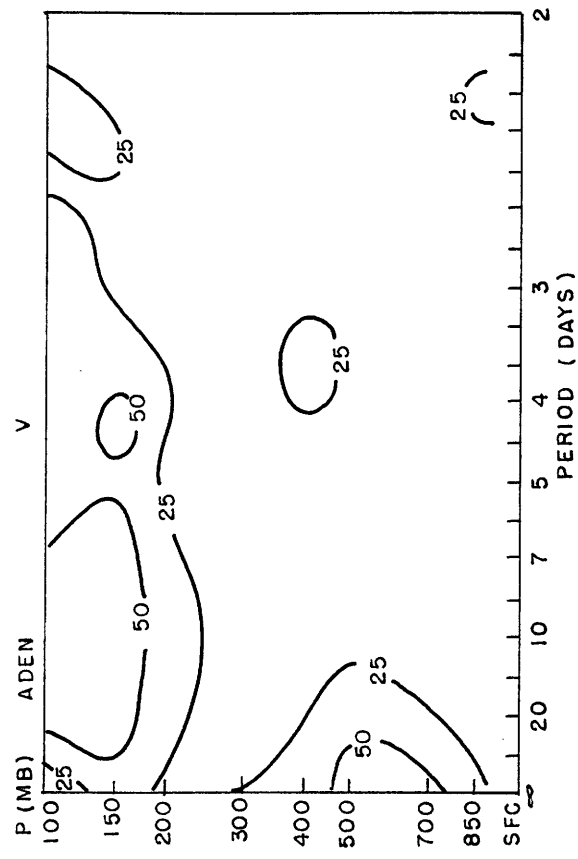


Fig. 4.1. Power spectral density estimates ( $m^2sec^{-2}$  day) of zonal and meridional wind as a function of pressure for the seasonal time series.

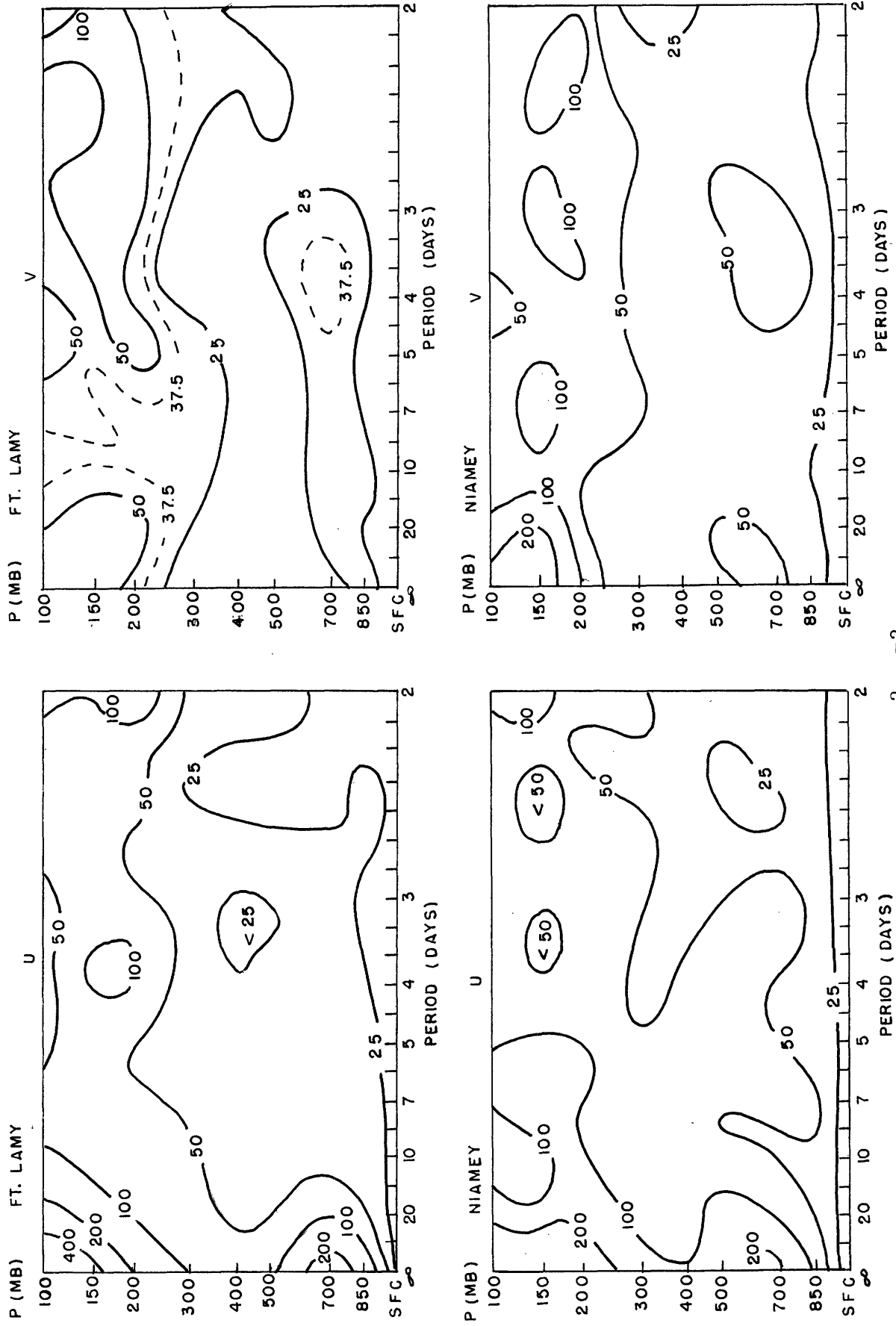


Fig. 4.2. Power spectral density estimates ( $m^2 sec^{-2}$  day) of zonal and meridional wind as a function of pressure for the seasonal time series.



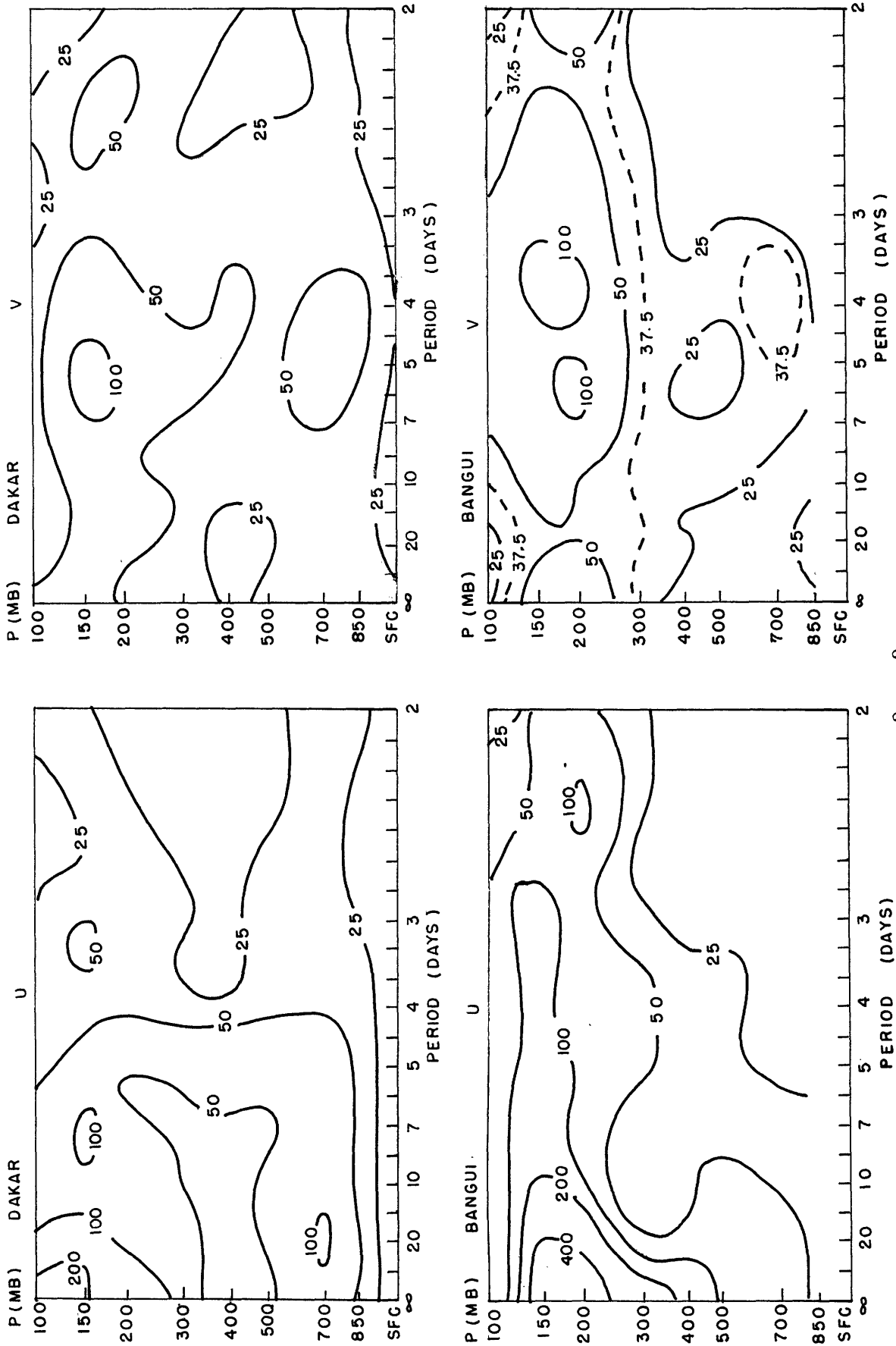


Fig. 4.3. Power spectral density estimates ( $\text{m}^2 \text{sec}^{-2} \text{day}$ ) of zonal and meridional wind as a function of pressure for the seasonal time series.

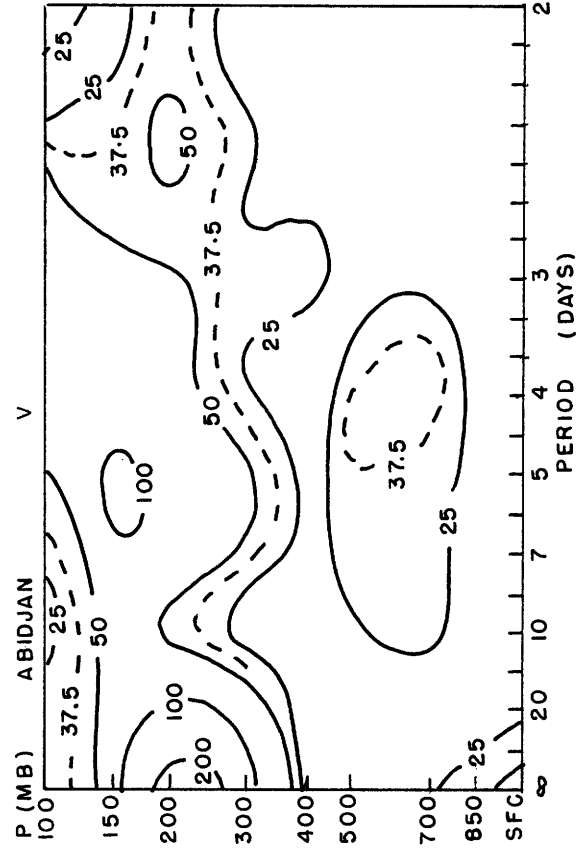
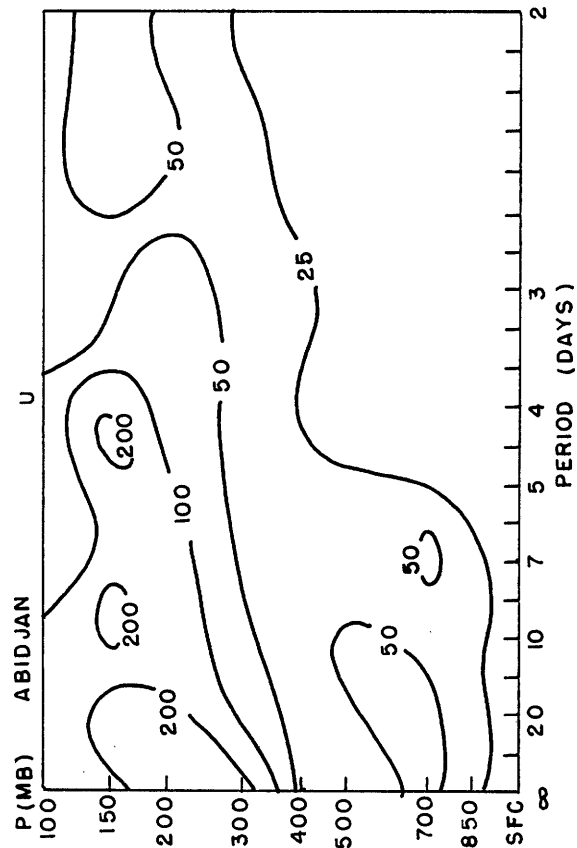
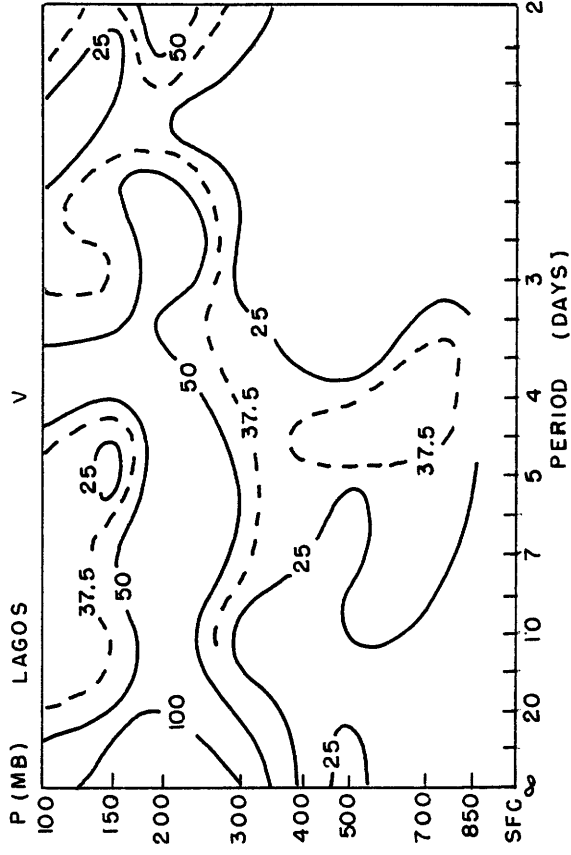
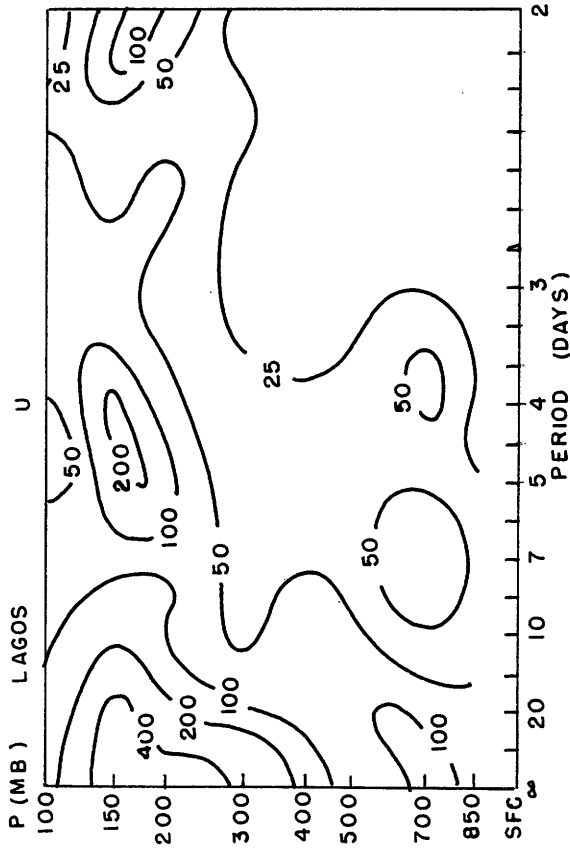


Fig. 4.4. Power spectral density estimates ( $m^2 sec^{-2}$  day) of zonal and meridional wind as a function of pressure for the seasonal time series.

700 mb in the lower troposphere and near 150 mb in the upper troposphere with an intermediate minimum close to 400 mb. This same tendency for relative maxima of the variance of the wind components to occur in the lower troposphere and near the tropopause has been noted in the equatorial Pacific by several authors (see e.g. Yanai et al, 1968). Most of the African stations have spectral peaks in the upper troposphere. It seems unlikely, however, that zonally propagating disturbances are producing most of the variance in the upper troposphere, since there is a lack of compatibility between the periods of the spectral peaks at adjacent stations. Perhaps much of the variance is the result of errors in the data. The one exception is the  $v$  spectral peak with a period of approximately five days near 150 mb, which probably represents the westward propagating waves observed near the equator in the vicinity of the tropopause and discussed by Yanai and Maruyama (1966). Although the amplitude of the disturbances in the upper troposphere is generally greater than that in the lower troposphere, the kinetic energy per unit volume at the 700-mb level is greater than that at 150 mb.

#### 4.4.4 The Source Region of African Waves

The results of subsequent sections show that the  $v$  spectral peak in the lower troposphere at periods of 4-5 days is caused by zonally propagating disturbances and that the wavelength, rate of propagation and seasonal occurrence of these disturbances are similar to the characteristics of African waves described by Carlson (1969a,b). He (1969b) has shown that African waves influence all of the stations used in this study except Aden and Khartoum which are east of his data network in a

region insufficiently populated with observations for conventional synoptic analysis. In order to determine whether Aden and Khartoum are also regularly influenced by easterly waves, the %TV for the seasonal series of the meridional winds was computed for each station from the surface to 100 mb (table 4.1) and compared to the results of the experiments with the random numbers summarized in table 3.2. The %TV is consistently a maximum value at 700 mb, where the amplitude of the wave motion is also greatest. At those stations where African waves have been synoptically observed the %TV of the 700-mb meridional wind is more than three standard deviations greater than the appropriate value from table 3.2. While %TV may not be normally distributed except for time series of pure white noise, its distribution with the addition of some redness is sufficiently close to normal that values more than two standard deviations from the mean can be considered to be highly significant. The significance is enhanced if a consistent pattern is observed between nearby stations. Though significantly large values of %TV occur most often at 700 mb, other levels evidently become affected to the west of Ft. Lamy. For example, although only the 700-mb v component at Ft. Lamy has a %TV significantly different from the random value, Dakar (which is more than 3000 km downstream from Ft. Lamy) has a significant %TV at all levels from the surface to 300 mb.

At Aden and Khartoum the values of %TV for v at each level (except 400 mb at Aden) depart by less than two standard deviations from the number which would be expected by chance. Even though there is a weak relative maximum in the spectra of the 700-mb v component

Table 4.1

Statistics for seasonal calculations of meridional wind  
 One-day lag autocorrelation (p), %TV and the number of standard deviations (N)  
 by which the %TV differs from the appropriate value in table 3.2.

	Aden			Khartoum			Ft. Lamy			Niamey		
	p	%TV	N	p	%TV	N	p	%TV	N	p	%TV	N
sfc	-	-	-	.35	34.5	1.9	.09	29.2	-1.4	.04	39.9	1.8
850	.05	32.9	-0.3	.36	31.9	1.3	.09	37.7	1.2	-.02	40.6	2.0
700	.27	27.1	-0.9	.40	29.2	0.8	.02	46.2	3.6	.03	49.8	4.8
500	.42	29.7	1.2	.12	38.1	1.1	-.13	35.0	0.5	-.03	36.2	0.6
400	.23	42.4	3.2	.07	37.6	1.1	.01	35.2	0.2	-.02	39.2	1.6
300	.17	38.1	1.6	.06	30.9	-0.9	-.00	33.7	-0.2	.07	36.0	0.7
200	.26	34.4	1.1	.17	29.0	-1.1	-.08	34.2	0.1	-.11	37.0	1.0
150	.23	33.3	0.5	.29	29.7	0.0	-.02	31.1	-0.9	.04	31.8	-0.7
100	.08	29.7	-1.2	.16	30.1	-0.8	.02	34.2	0.0	.21	28.0	-1.1

	Dakar			Bangui			Lagos			Abidjan		
	p	%TV	N	p	%TV	N	p	%TV	N	p	%TV	N
sfc	.18	43.1	3.1	-	-	-	-	-	-	.53	19.4	-1.4
850	.14	46.4	4.0	.18	42.3	2.9	.03	48.7	4.4	.20	42.7	3.1
700	.08	46.0	3.7	.13	51.4	5.4	.08	51.3	5.2	.14	50.4	5.2
500	.01	42.7	2.3	.13	44.0	3.2	.15	39.1	1.8	.15	46.6	4.1
400	-.01	51.2	5.2	.09	34.5	0.2	.09	45.3	3.5	-.06	43.1	2.8
300	.10	41.4	2.3	.10	35.8	0.7	.22	35.1	1.0	.32	33.5	1.3
200	.10	36.2	0.7	.01	46.4	3.7	.21	32.6	0.2	.19	36.4	1.2
150	.12	43.1	2.9	.04	44.1	3.1	.19	33.5	0.4	.19	48.8	4.9
100	.14	33.7	0.2	-.03	51.6	5.3	.07	38.9	1.5	-.08	45.5	3.5

at Khartoum, the %TV is still approximately the value to be expected in the absence of regular easterly wave passage. The value at 400 mb is significant at Aden, but the data show no coherence with the stations to the west. Perturbations in the meridional wind, therefore, are not related to any zonally propagating disturbances which regularly reach Africa. The variance characteristics of the seasonal time series of the meridional wind at Aden and Khartoum are sufficiently like the random number series that African waves did not normally influence these stations from 1960 to 1964. Since there is no reason to suppose that Aden and Khartoum are unrepresentative of the latitude band of easterly wave activity, no easterly waves regularly occurred east of 30°E.

The usual source region of African waves is thus limited to the region between Ft. Lamy and Khartoum; these stations are separated by approximately 1500 km. Carlson (1969b) has documented the likely origin of waves farther to the west and undoubtedly some waves form to the east of Khartoum, but the area between Ft. Lamy and Khartoum is the preferred source region.

The same calculations were made with the monthly time series of the meridional wind from 850 to 500 mb (table 4.2). From June to September the monthly time series support the contention that the African waves originate to the west of Khartoum; however, August is the only month when all of the stations to the west of Khartoum are clearly influenced by African waves. The number of degrees of freedom of the calculation of %TV for the monthly series is less than half that for the seasonal series and the computed standard deviation of the %TV

Table 4.2  
 Statistics for monthly calculations of meridional wind.  
 One-day lag autocorrelation (p), %TV and the number of standard deviations (N) by which  
 the %TV differs from the appropriate value in table 3.3.

	June						July								
	p	v 850 %TV	N	p	v 700 %TV	N	p	v 850 %TV	N	p	v 700 %TV	N	p	v 500 %TV	N
Aden	.50	39.3	1.8	.34	33.1	-0.6	.33	40.1	0.6						
Khartoum	.34	35.8	-0.1	.29	32.1	-1.1	.14	37.1	-0.8						
Ft. Lamy	-.10	44.2	0.5	.14	41.3	0.0	.01	39.6	-0.5						
Niamey	-.11	48.8	1.5	.15	48.5	1.5	-.00	43.2	0.7						
Dakar	.37	52.9	3.6	.22	50.7	2.2	.22	37.0	-0.6						
Bangui	.09	47.6	1.2	.23	48.5	1.8	.12	46.3	1.0						
Lagos	-.19	49.0	1.7	.12	72.0	6.2	.03	56.4	3.0						
Abidjan	.14	49.1	1.6	-.05	61.6	4.0	.00	53.4	2.3						
Aden	.28	49.1	2.1	.14	36.4	-0.9	.37	31.7	-0.7						
Khartoum	.16	43.6	0.6	.42	31.3	-0.4	.23	36.1	-0.6						
Ft. Lamy	.02	40.0	-0.4	.09	44.1	0.5	-.16	37.3	-0.7						
Niamey	.09	46.1	0.9	-.03	63.5	4.4	.06	36.8	-1.0						
Dakar	-.08	57.3	3.2	-.06	53.0	2.3	-.05	55.3	2.7						
Bangui	.21	43.8	0.8	.07	40.9	-0.2	.07	44.3	0.5						
Lagos	.17	63.1	4.5	.08	62.4	4.2	.15	56.6	3.1						
Abidjan	.17	65.0	4.9	.13	53.7	2.5	.10	43.9	0.5						

Table 4.2 (contd)

	August						September								
	p	v 850 %TV	N	p	v 700 %TV	N	p	v 850 %TV	N	p	v 700 %TV	N	p	v 500 %TV	N
Aden	-.06	33.0	-1.8	.27	26.8	-2.3	.30	42.4	0.9	.30	42.4	-2.3	.43	35.8	0.5
Khartoum	.22	48.0	1.6	.51	27.2	-0.4	.11	51.0	1.9	.17	45.5	1.0	.10	42.6	2.2
Ft. Lamy	.14	43.8	0.5	.00	58.9	3.5	-.12	44.1	0.5	-.01	45.6	0.7	-.01	42.8	0.2
Niamey	-.11	51.8	2.1	.04	58.5	3.4	.01	53.9	2.4	.06	44.2	0.5	.07	49.8	1.6
Dakar	.20	46.9	1.3	.06	51.8	2.0	.04	49.0	1.4	.18	51.1	1.9	.12	54.0	2.6
Bangui	.20	54.2	2.8	.16	66.8	5.4	.19	52.3	2.4	.08	65.0	4.7	-.04	56.2	2.9
Lagos	.08	56.7	3.0	.20	65.6	5.1	.24	46.9	1.5	-.14	55.5	2.9	-.10	44.2	0.5
Abidjan	.18	48.1	1.5	.27	61.9	4.6	.18	58.5	3.6	-.12	56.1	3.0	.12	48.5	1.4
Aden	.09	43.8	0.4	.34	44.7	1.6	.34	43.8	0.4	.34	44.7	1.6	.43	35.8	0.5
Khartoum	.32	31.8	-1.0	.17	45.5	1.0	.17	31.8	-1.0	.17	45.5	1.0	.10	42.6	2.2
Ft. Lamy	-.02	43.0	0.2	-.01	45.6	0.7	-.01	43.0	0.2	-.01	45.6	0.7	-.01	42.8	0.2
Niamey	-.00	43.2	0.2	.06	44.2	0.5	.06	43.2	0.2	.06	44.2	0.5	.07	49.8	1.6
Dakar	.21	50.1	2.0	.18	51.1	1.9	.18	50.1	2.0	.18	51.1	1.9	.12	54.0	2.6
Bangui	.15	44.2	0.6	.08	65.0	4.7	.08	44.2	0.6	.08	65.0	4.7	-.04	56.2	2.9
Lagos	-.04	57.2	3.1	-.14	55.5	2.9	-.14	57.2	3.1	-.14	55.5	2.9	-.10	44.2	0.5
Abidjan	.26	47.4	1.5	-.12	56.1	3.0	-.12	47.4	1.5	-.12	56.1	3.0	.12	48.5	1.4



is fifty per cent larger for the monthly series. This makes the significance criteria for the monthly series more difficult to exceed. Perhaps wave activity is more uniform in August and thus is able to exceed the criteria. Apparently a longer data sample is needed for a thorough analysis of the monthly series.

#### 4.2.3 Vertical Structure of the Waves as Determined from the Meridional Wind

Carlson (1969b) has indicated that the maximum amplitude of African waves occurs in the vicinity of 600 mb but the spectral results for only the mandatory levels reveal that the amplitude is greatest at 700 mb. It was decided, therefore, to calculate interlevel cross spectra within each station for the time series of meridional wind at all levels paired individually with the meridional wind at 700 mb. The resulting coherence and phase differences averaged for the periods from 3.1 to 5.7 days are shown in Fig. 4.5 for the stations along 15° N. The figure indicates that the depth of the atmosphere affected by the African waves increases steadily toward Dakar; moreover, a consistent pattern of phase differences shows that the 700-mb v component lags behind those at all other levels. This means that the trough axis of the average wave tilts toward the east with height up to 700 mb and toward the west above that level. On the assumption of thermal wind balance, this result implies relatively cold air behind the trough axis below 700 mb with warm air behind the trough axis above this level. This is compatible with the temperature structure to be expected from kinematic distortion of the zonal mean temperature field. Since the meridional

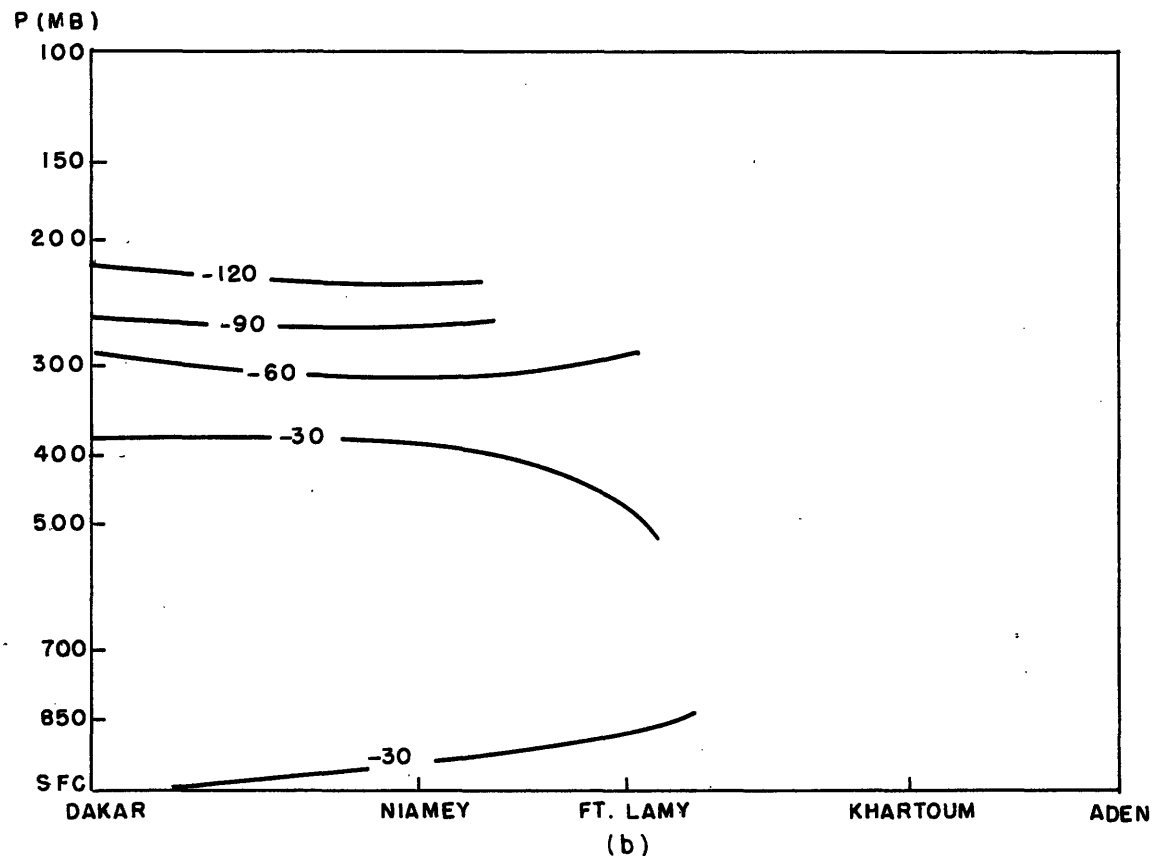
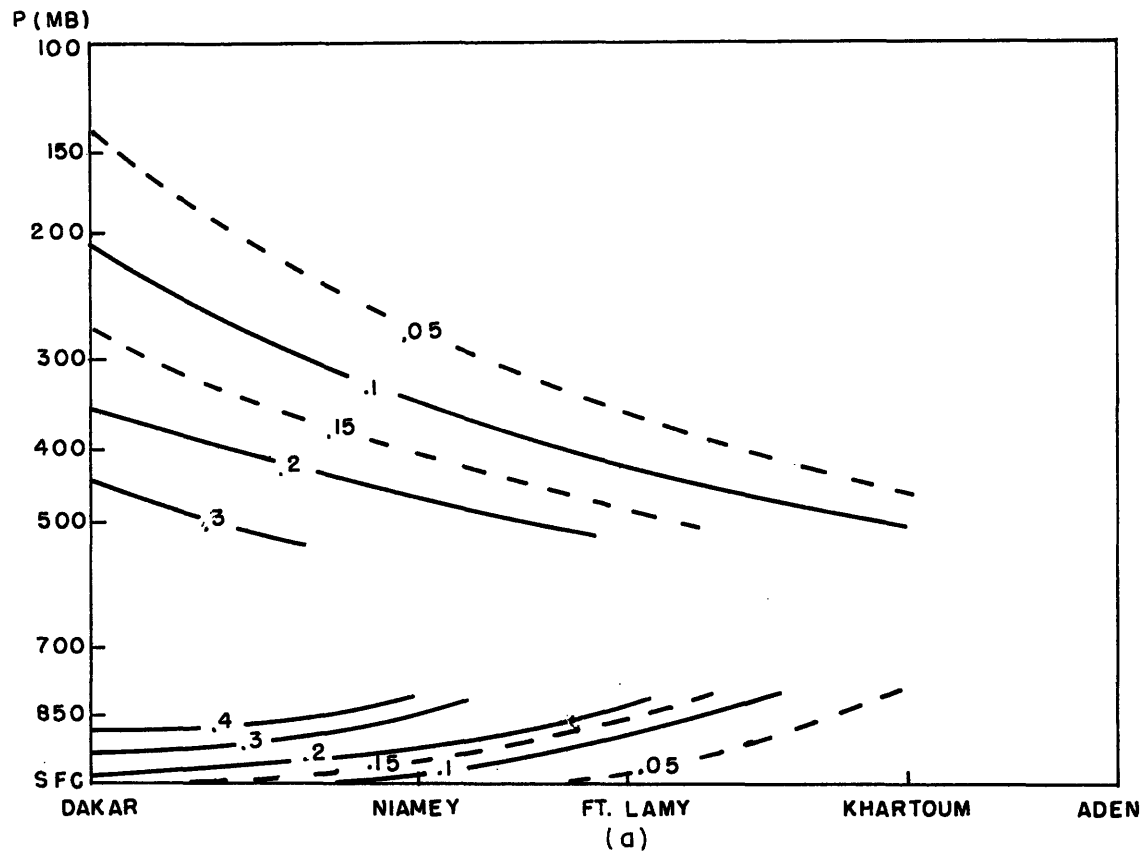


Fig. 4.5. Interlevel cross-spectrum results relative to 700 mb and averaged for periods from 3.1 to 5.7 days for the meridional wind, (a) coherence and (b) phase difference in degrees where negative values indicate that the 700-mb level lags behind the second pressure level.

gradient of zonal mean temperature reverses at about 600 mb near 10-15° N, the southerly winds which occur east of the trough axis produce cold advection below 600 mb and warm advection above. The tilt of the axis is similar at Lagos and Abidjan but at Bangui the axis slopes eastward with height throughout the lower troposphere.

#### 4.2.4 Vertical Influence of African Waves

The magnitude of the relationship between two time series is given by the cross spectral density function. Fig. 4.6 shows interlevel cross spectral density estimates of the meridional wind relative to 700 mb for selected stations. It is interesting to note that at those stations where easterly waves occur there is a correlation between these waves and disturbances in the upper troposphere with periods of approximately 4-5 days. This relationship increases toward Dakar as the wave grows vertically and is also enhanced toward the south. It appears likely that the African waves are contributing to the variance in the upper troposphere.

#### 4.2.5 Horizontal Wavelength of Waves

With the aid of both satellite pictures and conventional synoptic analyses at 10,000 ft Carlson (1969b) has estimated the horizontal wavelength of African waves to be about 2000 km for the summer of 1968. If the African waves were periodically propagating in the zonal direction during the summers from 1960 to 1964, the wavelength and direction of propagation of the disturbances can be estimated by systematic use of the phase difference between neighboring stations. Computations were

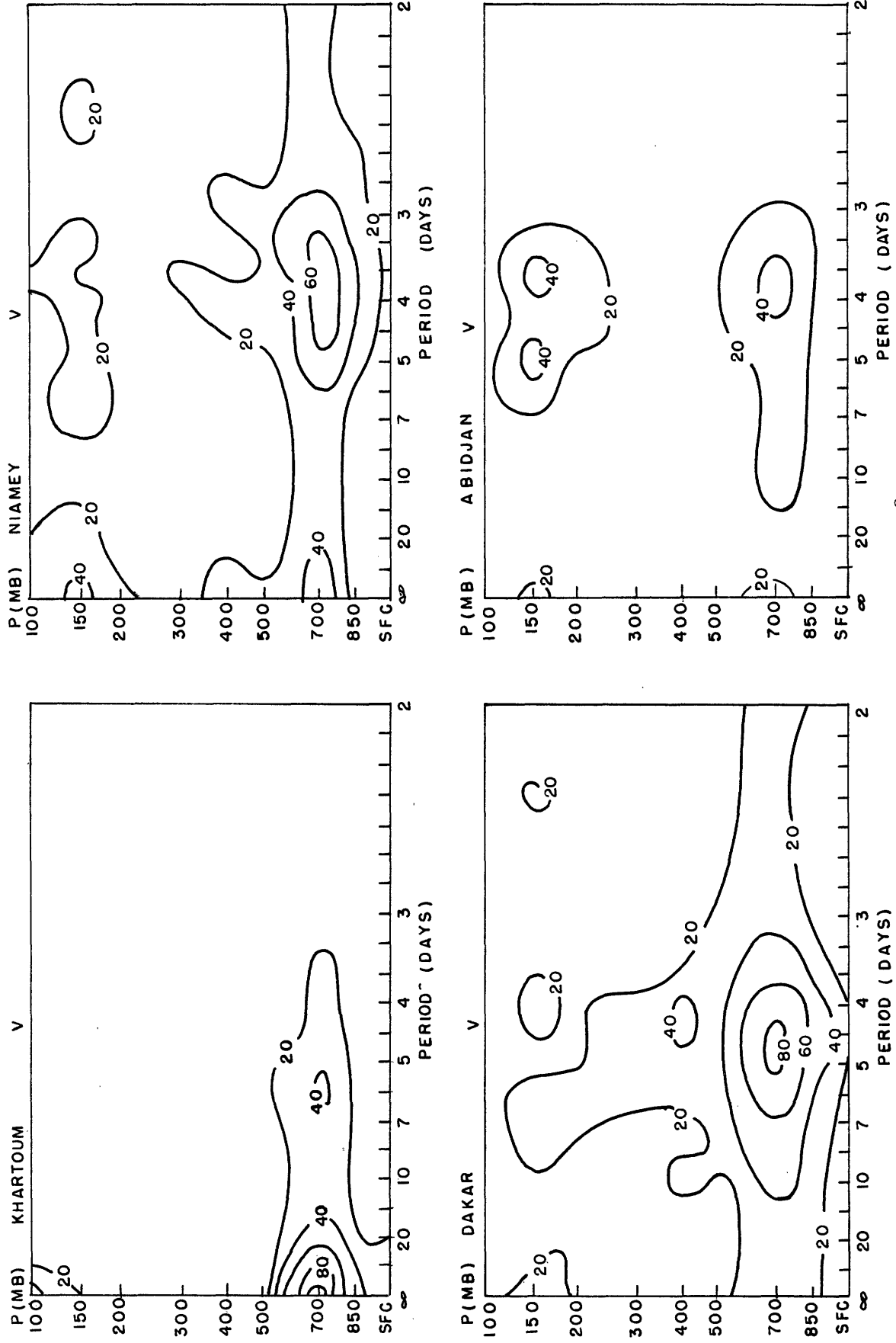


Fig. 4.6. Interlevel cross-spectral density estimates (m<sup>2</sup>sec<sup>-2</sup> day) relative to 700 mb and averaged for periods from 3.1 to 5.7 days for the meridional wind.

made of the coherence and phase difference between stations for the seasonal series of the 700-mb meridional wind. In Fig. 4.7 the phase difference  $(\Delta\theta)$  is plotted against the longitudinal separation  $(\Delta\lambda)$ ; these quantities are defined so that a disturbance propagating toward the west has positive  $\Delta\theta$  and  $\Delta\lambda$ . The values of the coherence are quite low and the  $\Delta\theta-\Delta\lambda$  relation shows some scatter but is approximately linear. Since a longitudinal separation of  $35-40^\circ$  is required for a phase difference of  $360^\circ$ , the wavelength can be crudely estimated to be 4000 km and the wave propagates toward the west. With the assumption that the average period is 4.5 days, the waves propagate toward the west at 9.5 m/sec. This is slightly slower than the average speed of the 700 mb zonal wind velocity.

The statistical estimate of the wavelength is larger than the synoptically observed wavelength of 2000 km just as the 4-5 day period of the peak in the spectrum is larger than the observed periodicity of 3.2 days (Carlson, 1969b). This discrepancy is also characteristic of the spectral results of Wallace and Chang (1969), Chang et al. (1970) and Nitta (1970a) who obtained estimates of the wavelength and period of easterly waves in the equatorial Pacific which are larger than synoptic observations in that region (Palmer, 1952). The larger estimates of the wavelength and period which have been computed with the power-spectrum methods may result because of the use of unrepresentative data; but it seems more likely that the discrepancy is due to a lack of uniformity of the waves. Brief interruptions of wave activity and variations of amplitude between successive waves can contribute to

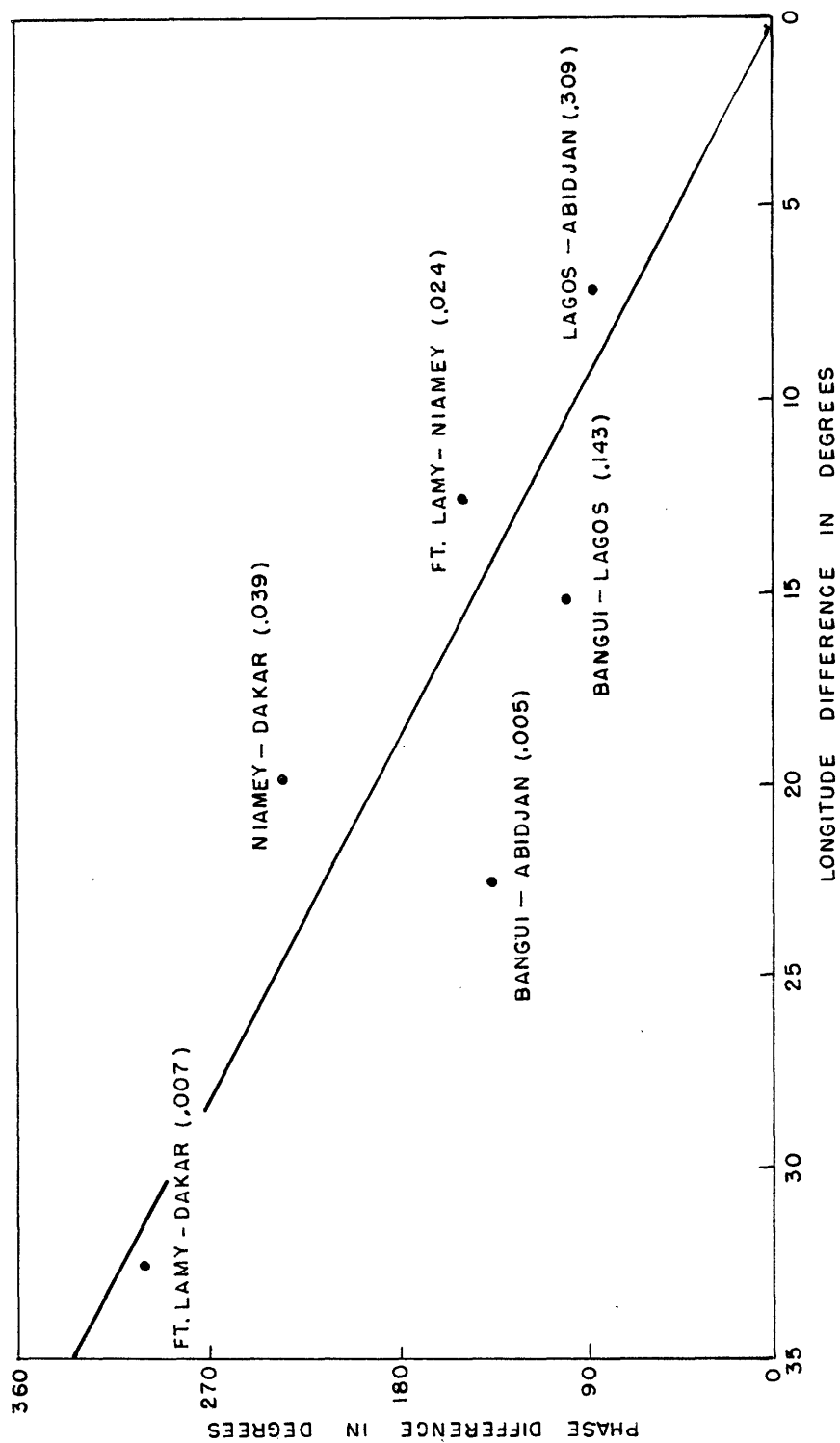


Fig. 4.7. Phase difference between the meridional wind fluctuations of African waves as a function of longitude separation between stations. Longitude separation is measured from the first station westward to the second station. Positive phase difference signifies that fluctuations at the first station lead those at the second station. The value of the coherence is in parentheses. The phase difference and coherence have been averaged over the periods from 3.1 to 5.7 days.

the larger spectral estimates of the wavelength and period.

#### 4.2.6 Horizontal Tilt of Wave Axis

The horizontal tilt of the trough axis can be investigated by computing the phase difference of the 700-mb v component for the seasonal series between stations along nearly the same meridian. This comparison can be made for two pairs of stations

<u>northern station</u>	<u>southern station</u>	<u><math>\Delta\lambda</math></u>	<u>phase lead of southern station</u>	<u>coherence</u>
Ft. Lamy (12°8'N, 15°2'E)	Bangui (4°23'N, 18°34'E)	3°32'	110°	.13
Niamey (13°29'N, 2°10'E)	Lagos (6°35'N, 3°20'E)	1°10'	55°	.06

When adjustment is made for the longitudinal difference of the stations, the southern portion of the wave at 5°N leads the central part of the wave near 13°N by about 1/6 of a wavelength. This result indicates that the axis of the disturbance is directed from southwest to northeast in the southern part of the zone of maximum African wave activity. Although the coherence values are too small to be significant, the similarity of the sign and magnitude of the phase difference gives credibility to the results.

There are no stations near 20°N which took observations regularly enough for spectral analysis to be applicable, therefore, nothing can be said concerning the horizontal tilt of the waves north of 13°N. The observed tilt of the wave between 5 and 13°N is such as to produce

an equatorward transport of easterly momentum away from the easterly jet if the flow is approximately nondivergent.

#### 4.2.7 Monthly Variations of Wave Activity

Carlson (1969b) and Frank (1970) indicate that easterly waves progress across Africa and into the Atlantic from mid June to early October. In order to investigate month-to-month variations of African waves the spectral density estimates for the 700-mb meridional wind at Niamey and Dakar are displayed in Fig. 4.8 for each month. These stations are chosen because they represent the region where the waves attain their maximum amplitude. A significant spectral peak near 4-5 days occurs from June to September but none during May, October and November. The lack of a spectral peak which can be associated with easterly waves during October probably implies that the waves occur for part of the month only. At both stations the period of maximum power spectral density is a minimum during August. Whether this is a random fluctuation in the data, an indication of a change in the preferred period in response to seasonal variations of the large-scale circulation, or a manifestation of more uniform wave propagation is not clear from an examination of the data. Evidence suggesting that this is not a random fluctuation has been given by Frank (1970) who found that the average frequency of waves passing Dakar during the years 1967 to 1969 reached a maximum near the first of August.



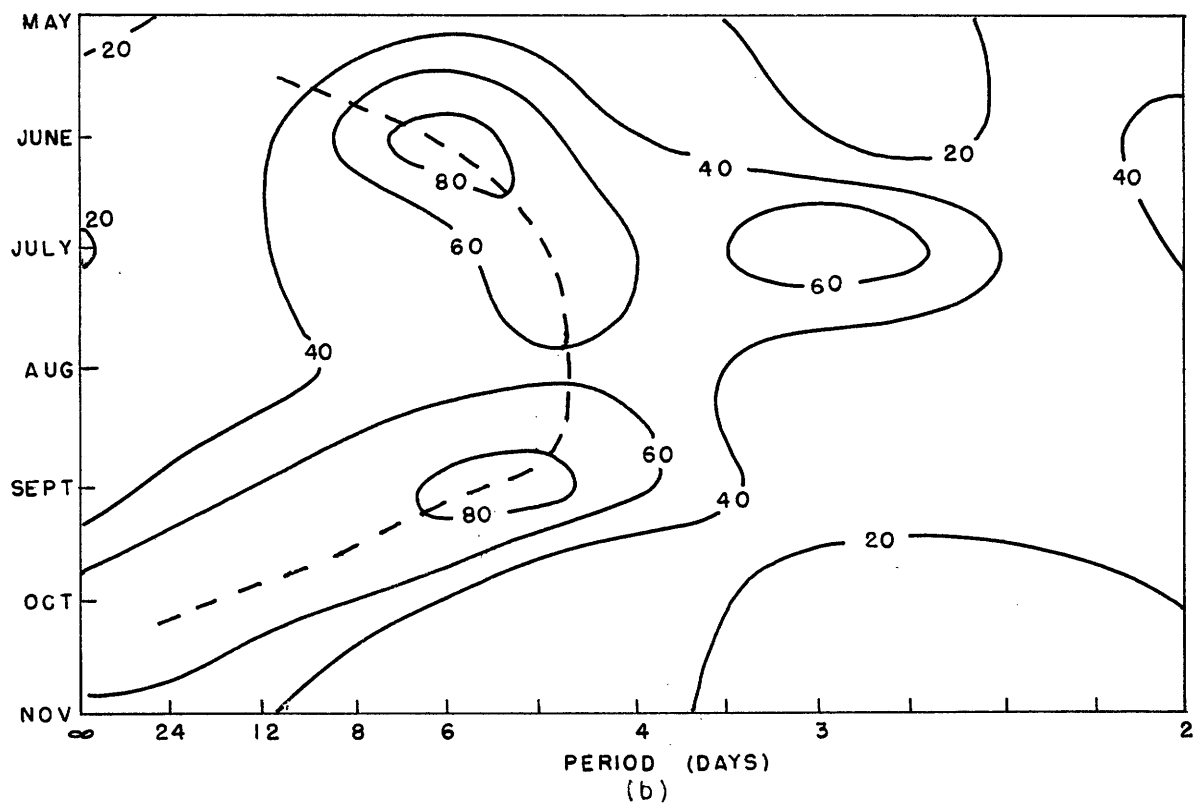
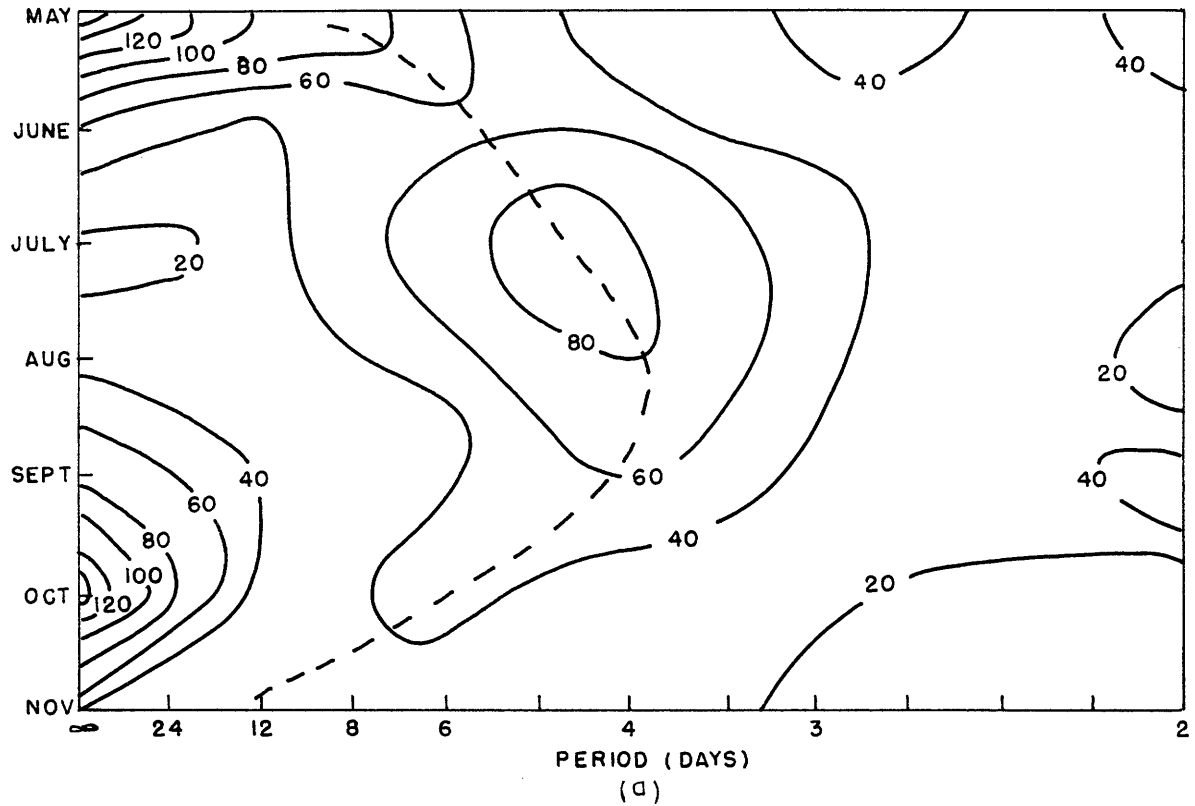


Fig. 4.8. Power spectral density estimates ( $\text{m}^2 \text{sec}^{-2} \text{day}$ ) of 700-mb meridional wind for monthly time series (a) Niamey and (b) Dakar, dashed line joins the peak spectral-density estimate.

#### 4.2.8 Seasonal Variations of Wave Amplitude

In both the Atlantic and Pacific Oceans the total number of hurricanes and tropical storms fluctuates greatly from year to year. Until recently it has been impossible to observe the annual number of African waves. For this reason yearly variations in wave activity could not be related to similar variations in the number of tropical storms. Frank (1970) has noted that although there was a considerable difference in the amount of tropical storm activity in the Atlantic from 1968 to 1969, this difference was not accompanied by any significant change in the number of African waves. While the number of African waves may not change much from one year to the next, their strength may vary from season to season. Such an effect has been documented in the Pacific where Wallace and Chang (1969) found an order of magnitude increase of variance in the lower tropospheric  $v$  components of easterly waves from 1963 to 1964. The increased amplitude of the easterly waves during 1964 may account for the unusual number of low-latitude tropical cyclones in the Pacific during 1964 (Chang et al., 1970).

Since most of the energy of the African waves is in the meridional wind component, the strength of the average wave should be proportional to the variance of  $v$ . Fig. 4.9 shows monthly values of the variance of the 700-mb meridional wind at Niamey and Dakar. The magnitude of the variance changes at most by a factor of two or three from one month to the next and no seasonal change is observed which compares to that which occurred in the Pacific between 1963 and 1964.

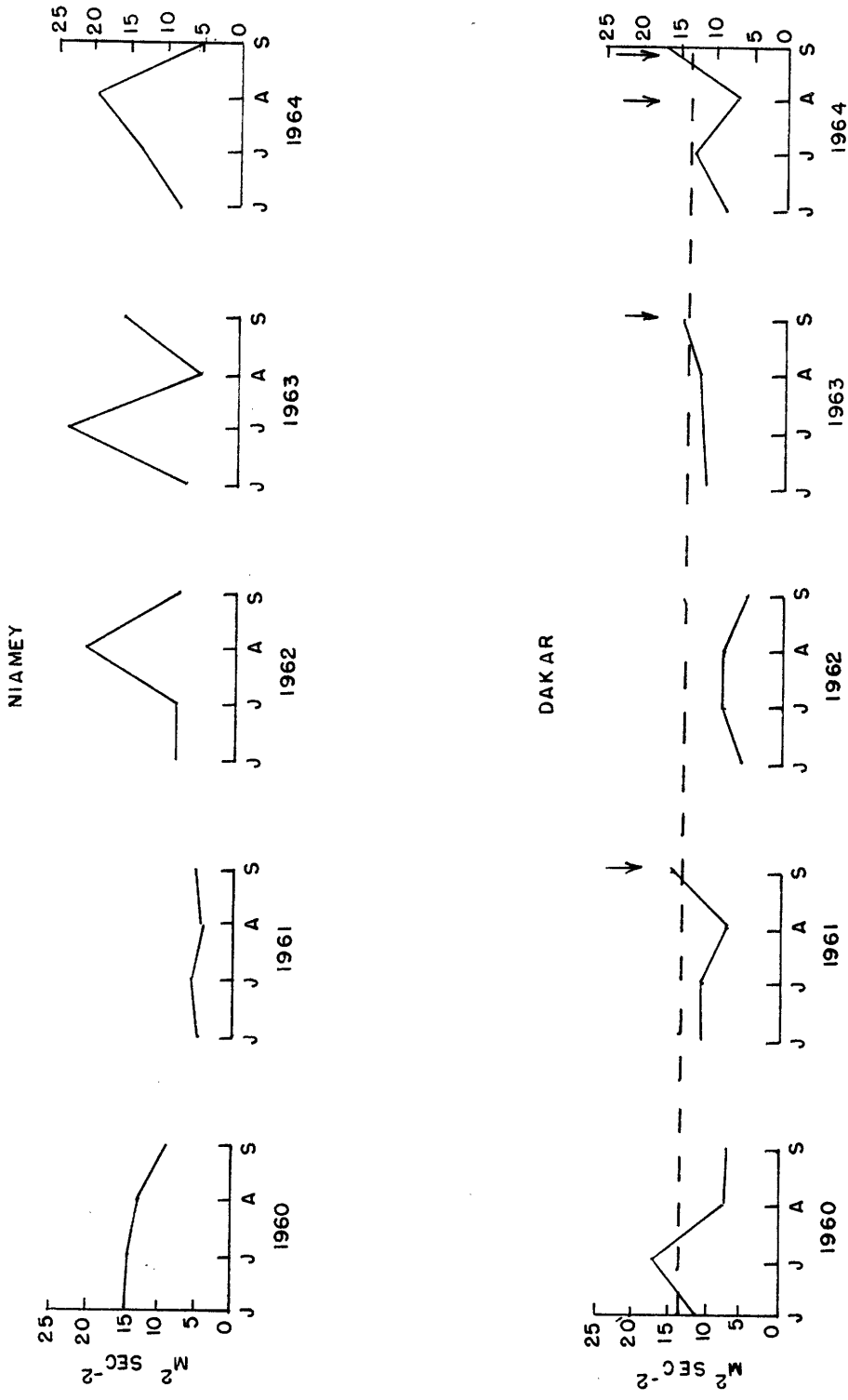


Fig. 4.9. Estimates of the variance of the 700-mb meridional wind in the period range 3.0 to 6.0 days; arrows indicate those months with four or more tropical cyclones in the Atlantic region.

Carlson (1969a) has stated that approximately half of the tropical storms and hurricanes which form during August and September are attributable to African waves. Although no relationship has been observed between minimum surface pressure or amount of convection of African waves and subsequent tropical cyclone development, it seems likely that the amplitude of a wave in the middle troposphere may be related to its ability to intensify.

Table 4.3 contains the number of hurricanes and tropical storms (both named and unnamed) which formed in the Atlantic region during each month from 1960 to 1964 and table 4.4 lists the estimated seasonal variance of African waves at Dakar and Niamey. These tables and Fig. 4.9 show that there is a tendency for the average 700-mb amplitude of the waves at Dakar to be greater than normal during those months and seasons when tropical cyclone frequency in the Atlantic is above average.

Table 4.3

Total number of tropical storms (named and unnamed) and hurricanes in the North Atlantic region.

	<u>June</u>	<u>July</u>	<u>August</u>	<u>September</u>	<u>October</u>	<u>November</u>	<u>July 15 to September 30</u>
1960	1	2	2	2	0	0	5
1961	0	1	0	5	2	2	6
1962	0	0	2	2	1	0	4
1963	0	1	1	5	2	0	7
1964	1	1	4	4	1	1	9

Table 4.4

Seasonal (July 15 to September 30) characteristics of 700-mb variance at Niamey and Dakar

	Niamey		Dakar		Deviation of Number of Storms from 5-Year Average
	Estimate of Variance	Deviation of Variance	Estimate of Variance	Deviation of Variance	
	3.1 to 5.7 Days	from 5-Year Average	3.1 to 5.7 Days	from 5-Year Average	
1960	12.7	+1.0	8.6	-2.5	-1
1961	4.9	-6.8	10.9	-0.2	0
1962	13.5	+1.8	10.5	-0.6	-2
1963	14.6	+2.9	13.3	+2.2	+1
1964	12.9	+1.2	12.4	+1.3	+3

### 4.3 Analysis of Temperature, Specific Humidity and Geopotential

#### Height

The structure of the waves was examined further by means of spectral analysis of the seasonal time series of temperature, specific humidity, geopotential height and surface pressure. Power spectra of these quantities were computed from the surface to 300 mb and intra-level cross spectra of  $T$ ,  $q$  and  $z$  (or  $p_{sfc}$ ) calculated relative to  $v$ . Table 4.5 lists the %TV of the  $T$ ,  $q$ ,  $z$  and  $p_{sfc}$  spectra at Niamey and Dakar where the waves are strongest and extend through the deepest layer. The power spectra of temperature and specific humidity do not show any consistent peak at periods near 4-5 days. The %TV of the geopotential height, however, is consistently higher than the appropriate value from the random number calculations while the %TV of the surface pressure is significant at both stations. An examination of the cross spectral calculations reveals a distinct relationship between variations of the meridional wind and geopotential height (Fig. 4.10) with the maximum height trailing the maximum southerly wind by 1/4 of a wavelength (table 4.6). The computed amplitude of the geopotential height at 700 mb at Dakar is 5 meters. Although this value seems very small, a recent study concerning the accuracy of radiosonde-measured heights by Lenhard (1970) indicates that this amplitude is capable of being resolved with radiosonde methods which were used from 1960 to 1964. The  $90^\circ$  phase difference between meridional wind and height suggests that the waves may be in geostrophic balance, a fact which is verified by a simple calculation with the geostrophic equation.

Table 4.5

Statistics for seasonal calculations

One-day lag autocorrelation (p), %TV and the number of standard deviations (N) by which the %TV differs from the appropriate value in table 3.2

	Temperature			Specific Humidity			Geopotential Height and Surface Pressure		
	p	%TV	N	p	%TV	N	p	%TV	N
sfc	.34	22.6	-1.7	.06	32.8	-0.3	.38	35.2	2.4
850	.41	29.4	1.1	.04	37.0	0.9	.39	36.0	2.7
700	.17	32.8	0.0	.09	32.5	-0.4	.39	31.1	1.3
500	.24	32.3	0.4	.28	30.3	0.0	.20	37.0	1.4
400	.18	25.7	-2.0	.18	28.6	-1.1	.16	34.1	0.4
300	.26	27.5	-0.9	.08	30.8	-0.9	.14	36.0	0.8

Niamey

	Temperature			Specific Humidity			Geopotential Height and Surface Pressure		
	p	%TV	N	p	%TV	N	p	%TV	N
sfc	.67	13.1	-0.4	.18	38.4	1.7	.50	36.8	4.5
850	.34	35.2	1.9	.20	27.5	-1.3	.43	29.6	1.3
700	.17	30.2	-0.7	.26	31.4	0.2	.47	25.6	0.7
500	.26	26.5	-1.0	.19	33.6	0.4	.31	26.4	-0.8
400	.36	26.2	-0.4	.14	31.7	-0.4	.33	26.7	-0.5
300	.44	27.8	1.0	.10	37.1	1.1	.35	27.4	-0.1

Dakar

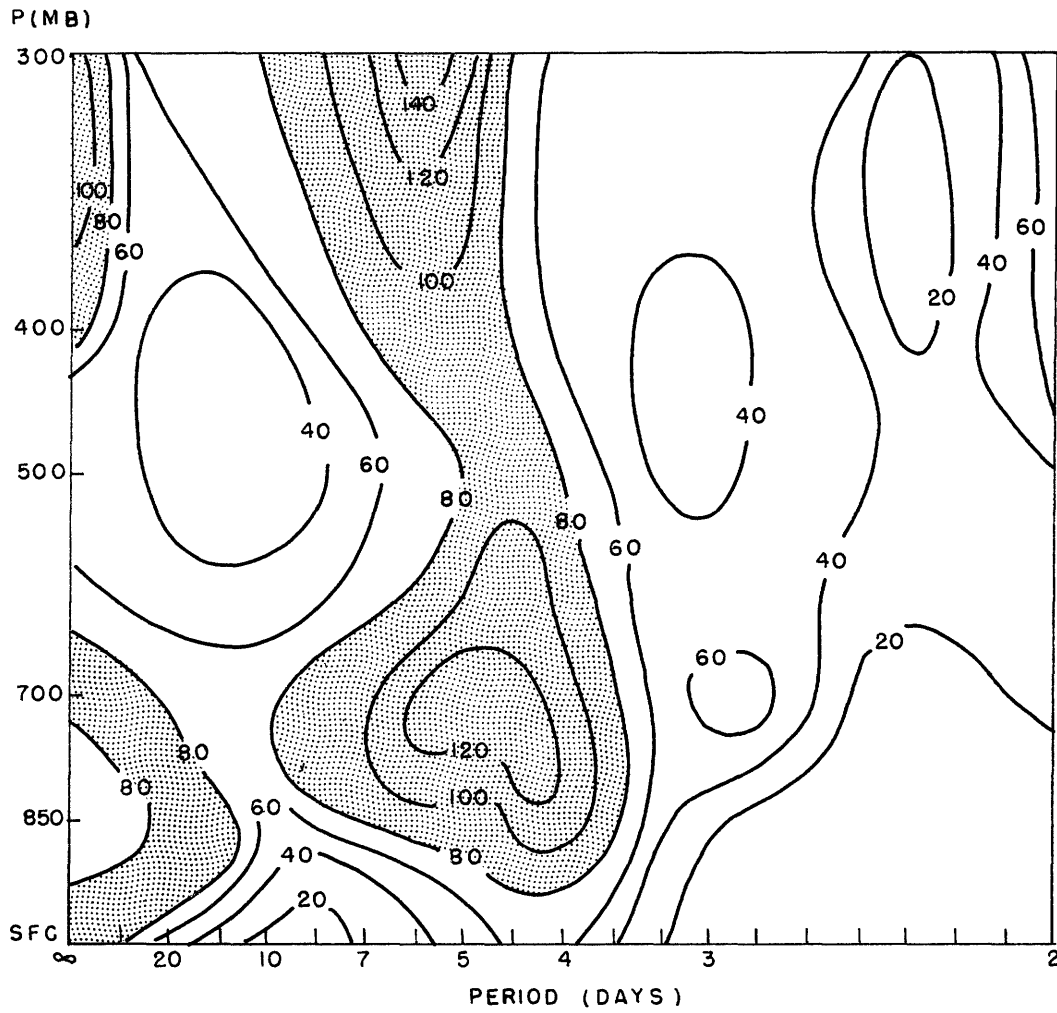


Fig. 4.10. Intralevel cross spectrum of meridional wind and geopotential height ( $\text{m}^2 \text{sec}^{-1} \text{day}$ ) at Dakar.



Table 4.6

Statistics for seasonal calculations of coherence and phase difference in degrees where  $-180 \leq \Theta < 180$ , cross spectra have been computed relative to the meridional wind.

		Niamey		Dakar			
	Temperature		Specific Humidity		Geopotential Height and Surface Pressure		
	Coherence	Phase Difference	Coherence	Phase Difference	Coherence	Phase Difference	
sfc	.03	146	.06	141	.07	88	
850	.14	-161	.01	-149	.22	92	
700	.06	158	.03	-49	.23	88	
500	.01	-32	.04	34	.11	93	
400	.01	175	.01	42	.06	101	
300	.00	135	.02	81	.02	93	
		Temperature		Specific Humidity		Geopotential Height and Surface Pressure	
	Coherence	Phase Difference	Coherence	Phase Difference	Coherence	Phase Difference	
	sfc	.01	157	.02	-162	.27	92
850	.13	-174	.12	27	.20	81	
700	.01	166	.11	-41	.35	80	
500	.04	-35	.17	-2	.12	92	
400	.04	-74	.09	5	.01	86	
300	.00	-161	.09	23	.07	113	

A similar relation also exists at Ft. Lamy and Niamey.

While the spectral technique does not identify significant temperature oscillations in association with the waves, it is possible to estimate the amplitude of the temperature fluctuations by means of the geostrophic thermal wind equation. At Dakar the temperature amplitude is estimated to be  $0.2^{\circ}\text{C}$  at 850 mb, which is the level of the maximum observed temperature variations. With allowance for the fact that the vertical derivative of the meridional wind is difficult to compute precisely, the amplitude of the temperature fluctuations should be no greater than  $0.4^{\circ}\text{C}$  and less than this value at those stations to the east of Dakar where the waves are not as well developed.

The reporting scheme for the temperatures on the data cards (card format 525 of the National Climatic Center) allocates only one column of the card for reporting the tenths digit of the temperature and dew point combined; this limits the temperature to an accuracy of about  $\pm 0.2^{\circ}\text{C}$ . In addition there is a random error of 0.3 or  $0.4^{\circ}\text{C}$  (Lenhard, 1970) in the method of observing temperatures with radiosondes. When communication errors are considered also, the amplitude of the errors is greater than the amplitude of the signal and it is not surprising that the temperature spectra do not reveal a significant peak at periods of 4-5 days. A consistent pattern is found, however, in the phase angle between meridional wind and temperature (table 4.6) which agrees with the structure inferred from the slope of the wave axis with height. From the surface to 700 mb  $v$  and  $T$  are out of phase indicating that cold air lies to the east of the trough axis but  $v$  and

T are in phase at 500 mb revealing that relatively warm air is east of the trough. The lack of any relationship between meridional wind and temperature in the upper troposphere results from the weakening influence of African waves above 500 mb.

Over the tropical oceans there is a characteristic sequence of weather associated with easterly waves: fair weather occurs a day or two in advance of the trough line and showery weather follows the passage of the trough line (see e.g. Riehl, 1945, and Palmer, 1952). Power spectral analyses of vertically averaged humidity in the equatorial Pacific by Wallace and Chang (1969) and Chang et al (1970) corroborate the observed convective pattern for oceanic easterly waves by revealing a distinct spectral peak at 4-5 days.

If either vertically averaged or constant-level specific humidity is an indicator of convection, it is difficult to draw any conclusions concerning the relation of convection to African waves from the statistical results with specific humidity. This is true also of synoptic observations and satellite pictures (Carlson 1969a, 1969b) which reveal that cloudiness becomes an organized part of the waves only after the waves have reached western Africa; but even in western Africa Carlson has found no preferred position of cloudiness relative to the trough axis. Immediately downstream from the source region of African waves the waves propagate horizontally without influencing the surface layer. During this time no organized cloud pattern is usually observed on satellite pictures. Apparently convection is not an important factor

in the formation of the African waves or in the maintenance of the waves east of the Greenwich meridian.

The lack of a consistent relation between convective cloudiness and the waves is somewhat surprising since it might be supposed that boundary layer convergence and large-scale ascent would promote organized convection in a manner similar to that observed in oceanic easterly waves. In the African waves warm advection and upward increase of cyclonic vorticity advection normally occur downstream from the trough axis in the lower troposphere. Quasigeostrophic reasoning indicates that upward vertical motion should be favored to the west of the trough line. The actual formation of clouds, however, is greatly confused because warm advection is accompanied by dry air.

#### 4.4 Horizontal Transports by African Waves

Computations of the horizontal eddy transports of zonal momentum and sensible heat were made for each month from May to November from the surface to 500 mb. The total horizontal eddy transport and the

contribution of the easterly waves in the period range from 3.0 to 6.0 days were calculated. The total horizontal eddy transport includes all turbulent eddy processes with periods less than a month; the effect of most lower frequency disturbances has been removed by subtracting the linear trend. The horizontal transport by eddies in the period range from 3.0 to 6.0 days (frequency range from 0.17 to 0.33 cycles per day) is estimated by

$$\overline{u'v'} = \sum_{f=.17}^{f=.33} C_{uv}(f) \Delta f$$

$$\overline{v'T'} = \sum_{f=.17}^{f=.33} C_{vT}(f) \Delta f$$

where the overbar represents averaging for a particular calendar month from 1960 to 1964,  $f$  is frequency,  $C(f)$  is the co-spectral density function and  $\Delta f = 0.042 \text{ day}^{-1}$ .

Since the time series are available at only eight stations, a detailed representation of horizontal transports as a function of latitude, longitude and height cannot be made; nevertheless, some inferences concerning the horizontal transports by African waves can be made by examining the covariances  $\overline{u'v'}$  and  $\overline{v'T'}$ . The similarity of the covariances at several stations suggested that they be averaged for Aden and Khartoum, for Ft. Lamy, Niamey and Dakar, and for Bangui, Lagos and Abidjan.

The sensible heat transports are shown in Fig. 4.11. In general the horizontal transport of sensible heat is negligible at the surface even at those stations within the baroclinic zone and is also negligible at all levels near  $5^{\circ}\text{N}$  (a region of weak zonal temperature gradient). At Ft. Lamy, Niamey and Dakar the heat transport is equatorward at 850 and 700 mb and weakly poleward at 500 mb both for African waves and all eddy motions. For these stations the direction of the transport is down the temperature gradient at each level above the surface.

As might be anticipated, the statistics for the covariance of  $u$  and  $v$  at each station depend on the position of the station relative to the mid-tropospheric easterly jet and the baroclinic zone at the surface. The number of upper-air stations is insufficient to determine the precise latitude of the jet axis; however, an examination of the monthly mean temperature maps and the monthly mean zonal winds at 700 mb suggests strongly that the jet axis is south of Ft. Lamy, Niamey and Dakar from October to June and north of these stations during July, August and September.

The horizontal transport of momentum is shown in Fig. 4.12 from which it is seen that momentum transports are quite small at the surface and 500 mb. At the stations near  $5^{\circ}\text{N}$  there is generally an equatorward flux of easterly momentum. There is, however, a poleward flux of easterly momentum at the 850-mb level at Ft. Lamy, Niamey and Dakar. This poleward transport of easterly momentum was also found at Tamanrasset ( $22^{\circ}47'\text{N}$ ,  $5^{\circ}31'\text{E}$ ) and Ft. Trinquet ( $25^{\circ}14'\text{N}$ ,  $11^{\circ}37'\text{W}$ ) in the  $\overline{u'v'}$  covariances for June to August which were computed by Professor

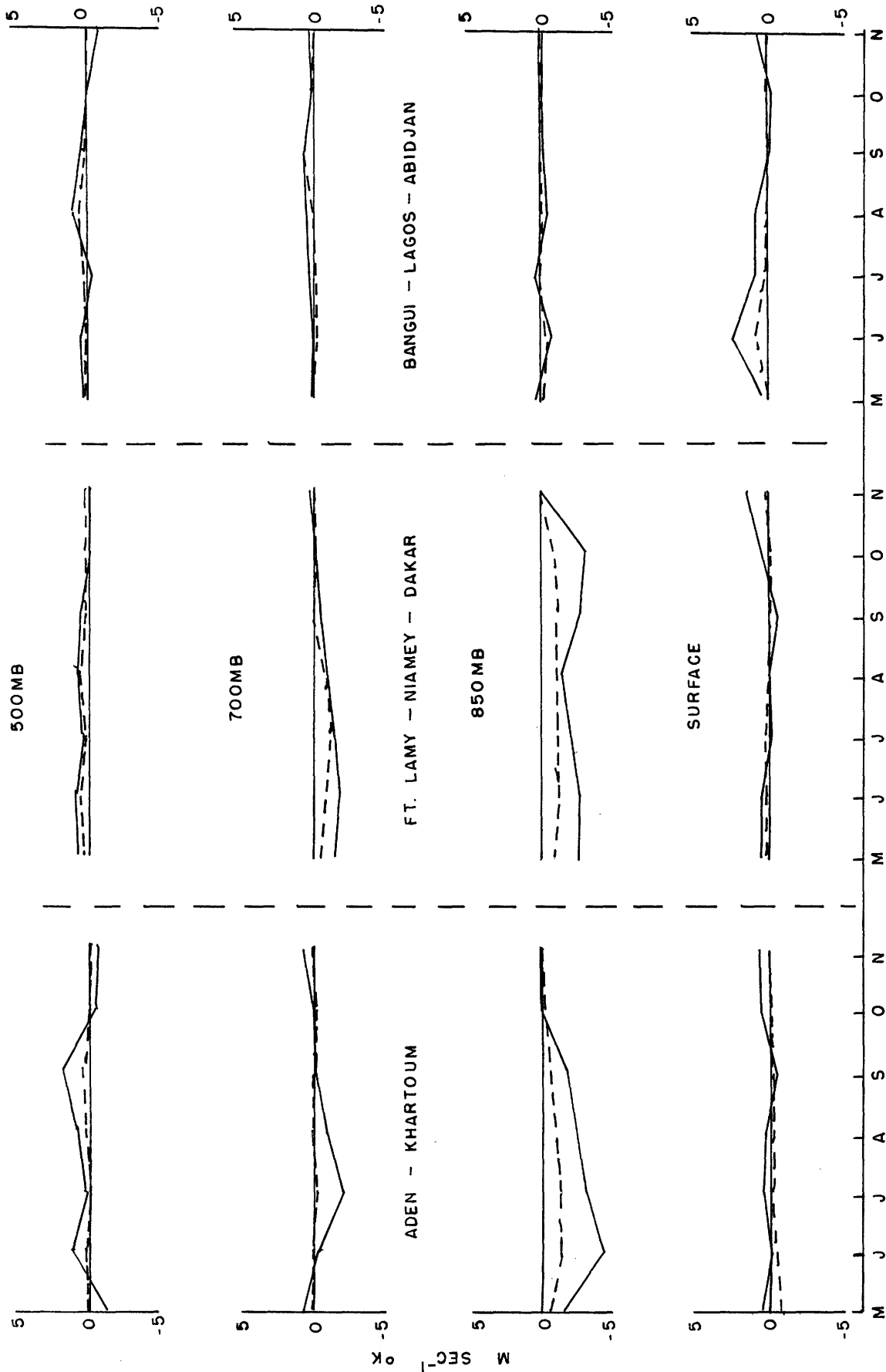


Fig. 4.11. Sensible heat transports computed from monthly time series; solid lines represent total eddy transport and dashed lines the transport of African waves.

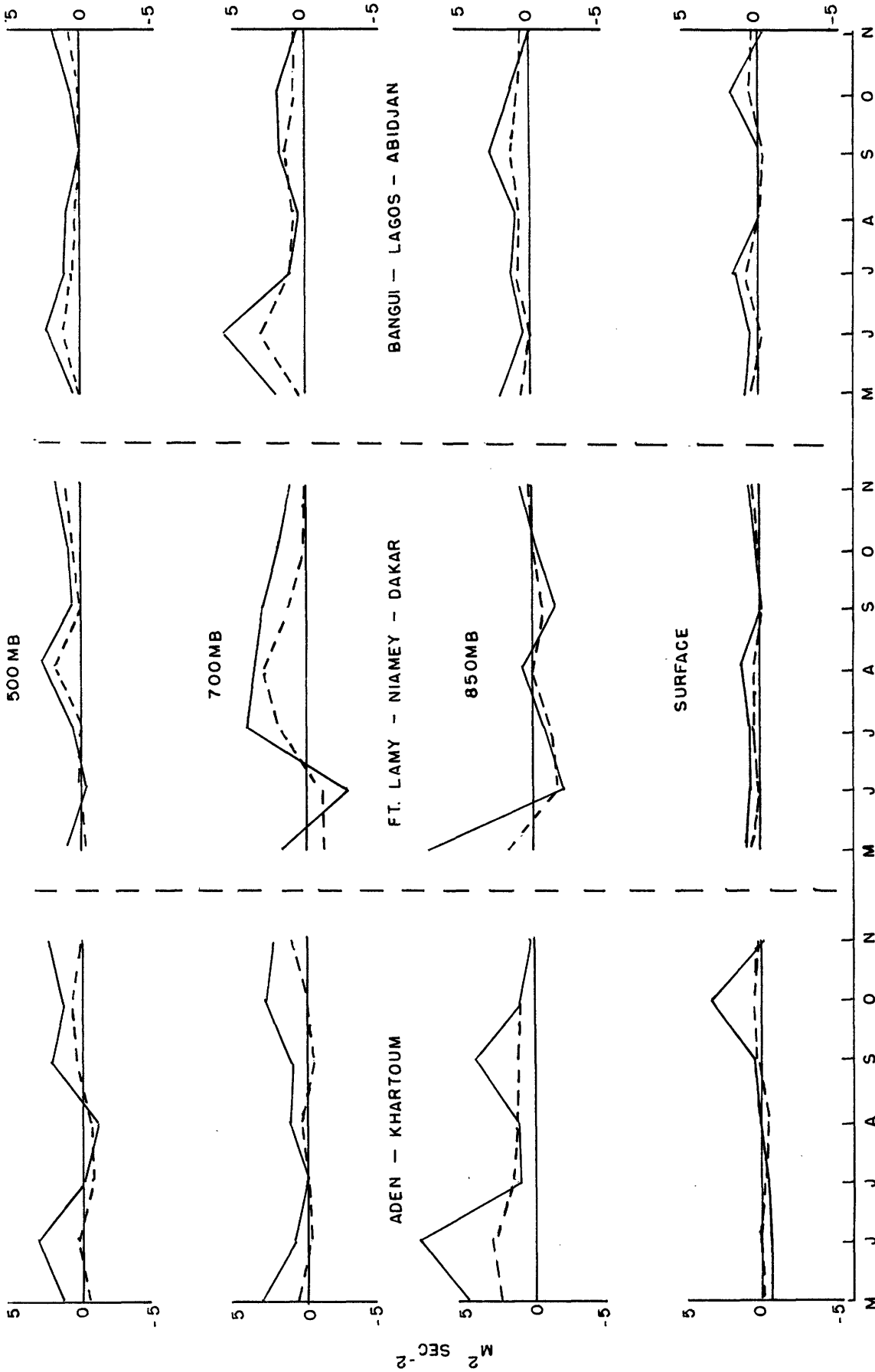


Fig. 4.12. Momentum transports computed from monthly time series; solid lines represent total eddy transport and dashed lines the transport of African waves.



R.E. Newell and students at MIT and may be related to the shallow, transitory thermal lows which have been frequently observed near the ITC over the Sahara in association with African waves (Carlson, 1969b). The magnitude of the momentum transport by African waves is largest at 700 mb at Ft. Lamy, Niamey and Dakar. At this level the direction of the transport changes from a poleward transport of easterly momentum in June to an equatorward transport of easterly momentum in July, August and September. This change occurs at each of the stations. As mentioned previously, the core of the easterly jet stream is south of these stations during June and north of them during the other months of easterly wave activity. Thus for each month from June to September the eddy motion is exporting momentum from the vicinity of the easterly jet; this confirms the direction of the momentum flux which was inferred from the southwest to northeast tilt of the 700-mb wave axis.

## Chapter 5

### Discussion of Possible Causes of African Waves

Speculations concerning the causes of African waves have been made by Carlson (1969b) and Frank (1970). Carlson suggested that the waves form as squall lines which are produced by afternoon heating over elevated regions and Frank felt that the waves originate from the mechanical effect of the easterly flow of air over the mountains of Ethiopia.

#### 5.1 Airflow Over Mountains

In the latitude band of  $10^{\circ}$ - $15^{\circ}$  N, where African wave activity is centered, there is an extended region of mountains in Ethiopia and a smaller mountain range near  $23^{\circ}$  E in the western Sudan (see Fig. 2.1). Near  $39^{\circ}$  E in Ethiopia there is a north-south ridge line which stretches from  $5^{\circ}$  to  $17^{\circ}$  N. To the west of this ridge line the mean meridional cross sections at  $35^{\circ}$  E show that during most of the African wave season the zonal winds are from the west up to 800 mb (6500 ft) and from the east above this pressure level. The elevation of much of the land in Ethiopia is over 6000 ft and many of the mountains are higher than 10,000 ft. The wind, therefore, is easterly only for those mountains which penetrate above 800 mb and is in the proper direction to account for westward propagating disturbances over North Africa.

In order to determine the role of the mountains in the generation of African waves the statistical results for Aden and Khartoum were examined. Khartoum is the only station immediately to the west of

Ethiopia which made a reasonably complete series of observations from 1960-1964. Observations from Malakal ( $9^{\circ}33'N$ ,  $31^{\circ}39'E$ ), which were available for only a limited time from 1964 to 1966, were used in the cross sections but were not taken frequently enough to be of value for spectrum analysis. Although Khartoum is located near the northern end of the Ethiopian mountains, it presumably would be affected by any periodic disturbances which might arise from airflow over the mountains. Aden is located just to the east of Ethiopia and has been used to examine the existence of wave motion in the 700-mb flow before it reaches the mountains. The absence of a significant peak in the power spectrum of the meridional wind at Aden (except the peak at 400 mb which is not coherent with any other station to the west) indicates that there are no waves in the easterly flow upstream from Ethiopia; moreover,  $\%TV$  at Khartoum is not significantly larger than that at Aden so that easterly waves do not arise immediately downstream from the mountains (table 4.1).

The mountains in the western Sudan between Khartoum and Ft. Lamy are generally 3000-5000 ft high. In the spring and fall the zonal wind is from the east near the mountain tops but during the African wave season the mountains are usually completely within the southwest monsoon. The airflow is not in the proper direction to produce the periodic disturbances which are propagating toward the west at Ft. Lamy.

Since these are the only mountain ranges in the area of African wave formation, airflow over mountain ranges cannot be responsible for the generation of African waves.

## 5.2 Squall Line Formation over Elevated Land Areas

On the basis of daily synoptic analyses Carlson (1969b) has estimated the longitude where each African wave was first observed during 1968. He found that half of the waves originated east of  $18^{\circ}\text{E}$  and that twenty per cent first appeared between  $10$  and  $12^{\circ}\text{E}$ . This source region between  $10$  and  $12^{\circ}\text{E}$  prompted Carlson to suggest that the waves may form as squall lines over the Cameroon Mountains; however, the longitude where a wave actually forms is not likely to be where the wave is first observed since the average  $v$  amplitude of the waves at 700 mb is only 1-2 m/sec. A second difficulty in the synoptic determination of the origin of these disturbances is the use of once per day analyses; this automatically introduces a westward bias in the longitude of the origin of the waves. While an occasional wave may form in the region between  $10$  and  $12^{\circ}\text{E}$ , it is unlikely that this area is an important source of African waves since an examination of the 700-mb wind statistics from 1960 to 1964 at Ft. Lamy indicates that the vast majority of the waves formed to the east of Ft. Lamy.

Squall lines, however, do develop regularly as the result of afternoon or evening convection over elevated ground of Cameroon and Nigeria and have been discussed by Eldridge (1957). These squall lines occur nearly every day, propagate westward at 15 m/sec and generally dissipate before traversing 500 miles. Since satellite pictures and statistical methods have not detected any relation of convection to the initial stages of wave development, it seems unlikely that African waves also form as the result of enhanced convection over mountains.

### 5.3 Barotropic Instability

During each month of African wave activity the waves transport easterly momentum away from the mid-tropospheric jet at 700 mb. The transport of easterly momentum away from the jet suggests that barotropic instability may be an important factor in the generation of African waves. In order to examine this possibility, meridional profiles of monthly mean absolute vorticity  $\left(-\frac{\partial u}{\partial y} + f\right)$  were computed for the 850, 700 and 500-mb surfaces from the cross sections at 5 and 35°E (Figs. 5.1 and 5.2). Although the stations are not sufficiently dense to determine the details of the horizontal shear of the zonal wind, at both meridians there is a clear indication of a maximum in the meridional profile of absolute vorticity which is most apparent at 700 mb and also occurs at 500 mb. A relative maximum in the absolute vorticity profile is a necessary condition for barotropic instability (see e.g. Nitta and Yanai, 1969) and is observed near 10-15°N during the same months that easterly waves occur. At 850 mb, however,  $-\frac{\partial u}{\partial y} + f$  is approximately a linear function of latitude. During November the relative maximum in the meridional profile of absolute vorticity is weaker and farther south at 5°E and from December to May it does not occur as a monthly mean phenomenon. The combination of relative maxima in the monthly mean profiles of absolute vorticity and the transport of momentum away from the easterly jet by the waves suggests strongly that barotropic instability is the source of energy for African waves.

Since the horizontal shear of the zonal wind increases by a factor of two from 35 to 5°E, the degree of barotropic instability also

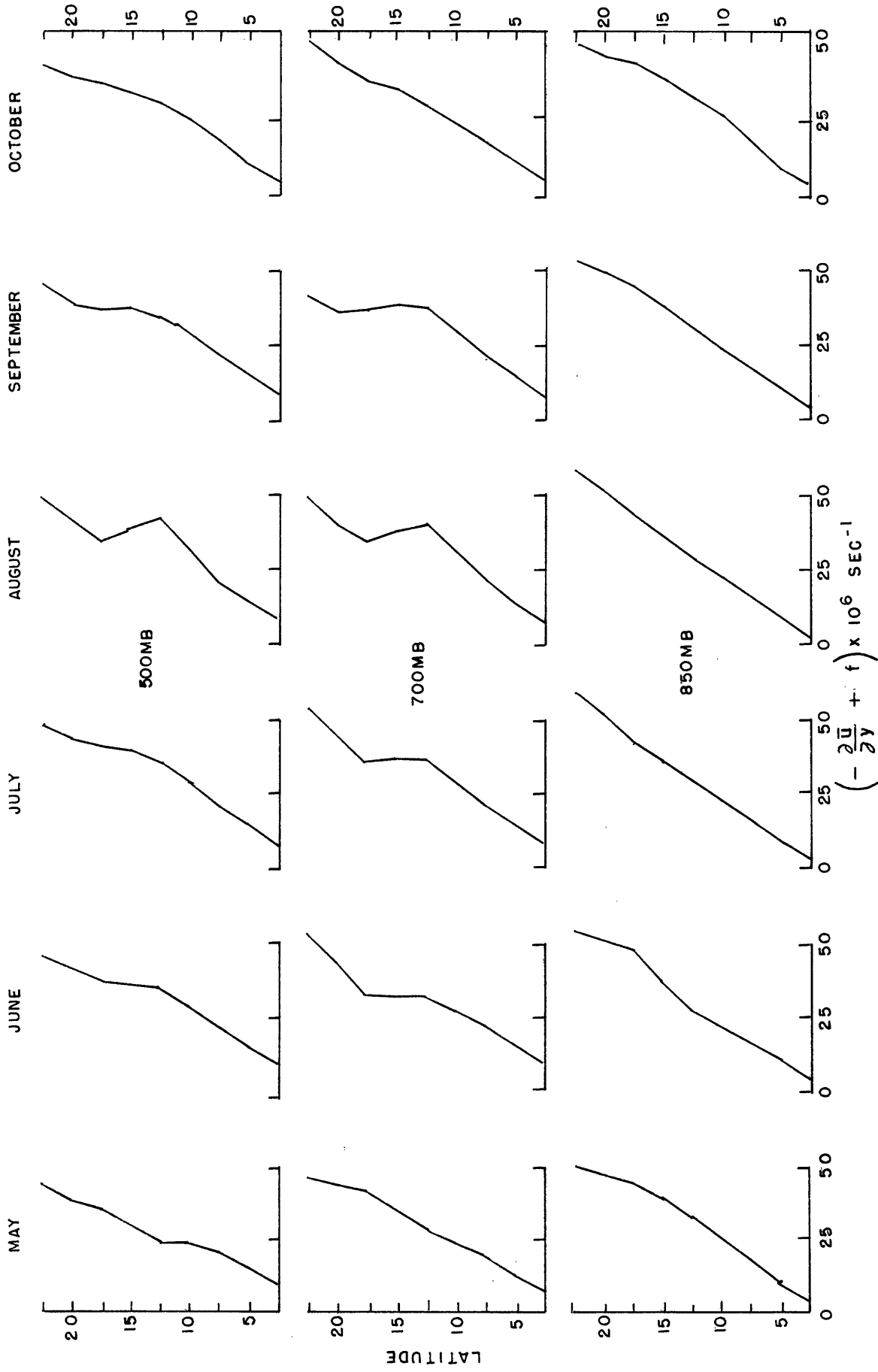


Fig. 5.1. Monthly mean absolute vorticity at 35°E.

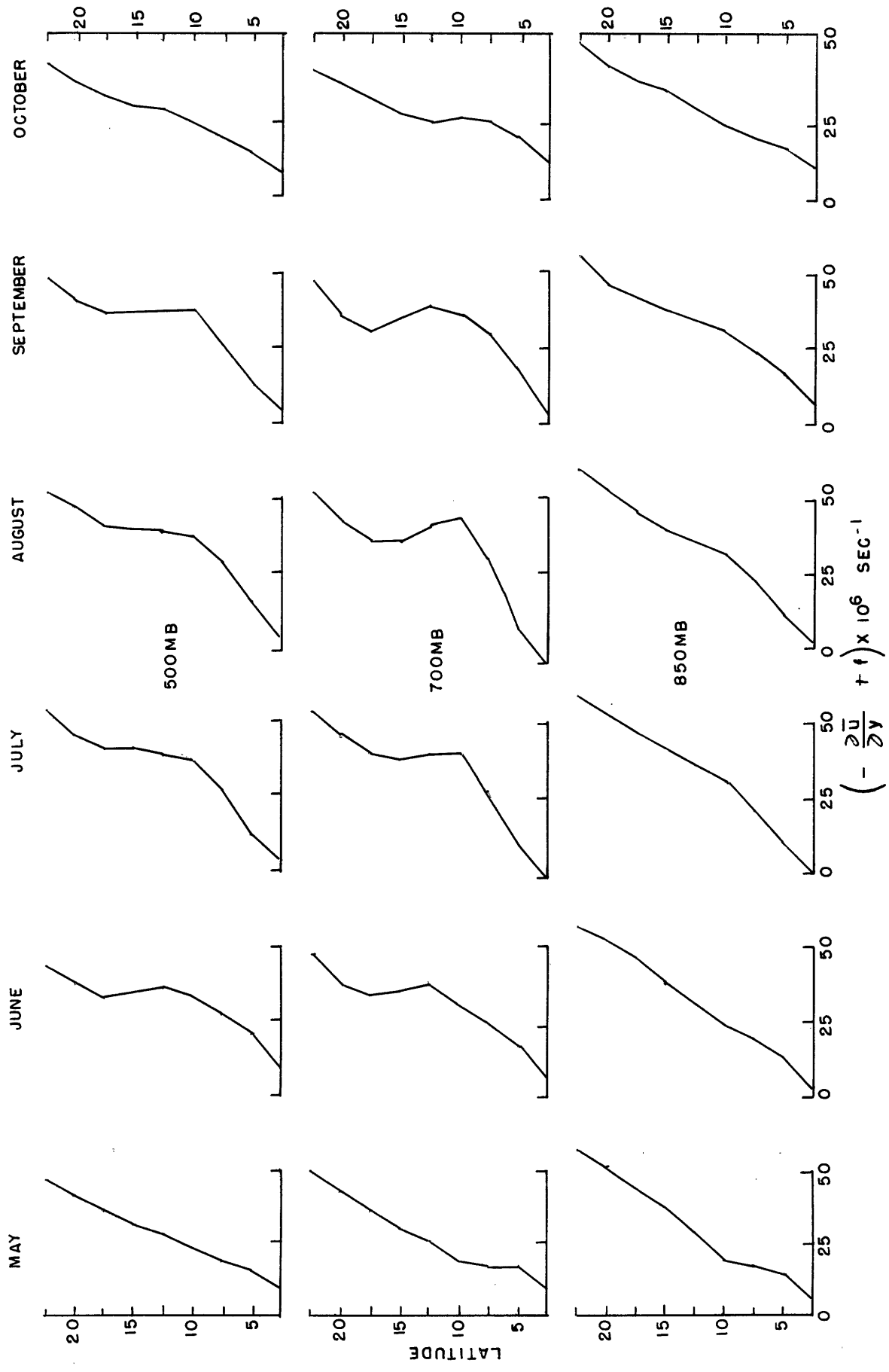


Fig. 5.2. Monthly mean absolute vorticity at 5°E.

increases between these longitudes. This may account for the fact that the source region of African waves is in east-central Africa rather than farther to the east.

The idea that barotropic instability may be the initial source of energy for tropical disturbances at low latitudes has been prevalent for many years (Yanai, 1961). Recent stability analyses with the linearized vorticity equation by Nitta and Yanai (1969) and Lipps (1970), both of which simulated conditions in the Marshall Islands region of the Pacific, have found that the wavelength of maximum growth rate is about 2000 km and the e-folding time is 5-7 days. The wavelength is very similar to that observed by Carlson (1969b) for African waves but the growth rate may be too slow to overcome the effects of friction. The mean zonal shear, however, of 12.6 m/sec between Niamey and Lagos for August at 700 mb is approximately double the shear considered in the numerical studies. Barotropic instability would undoubtedly yield a more reasonable growth rate if they had used a larger value of horizontal shear.

The 700-mb zonal wind component doubles in speed between Khartoum and Niamey (Fig. 2.8) even though this is the region where easterly waves are transporting momentum away from the mean zonal flow. If the 700-mb height field were aligned so that the heights at Khartoum were 5-6 meters higher than at Niamey, then the increase in wind speed could be explained by the flow of air down the height gradient; but the averaged heights at Khartoum, Ft. Lamy and Niamey differ by less than one meter and do not support the model of airflow down the height gradient. Since the surface isotherms, zonal flow and height fields



are oriented nearly east-west, a likely source of kinetic energy for the easterly flow is an ageostrophic meridional circulation in which warm air is rising and cool air sinking (Fig. 5.3). The meridional winds averaged from June to September at Khartoum, Ft. Lamy and Niamey (table 5.1) corroborate this model since there are southerly winds near the surface and in the upper troposphere with northerlies between these regions. The winds at Dakar do not follow this pattern but the 700-mb zonal wind at Dakar is less than that at Niamey, so the meridional circulation is not required. Note that Dakar is on the west coast of Africa and is not representative of stations in the baroclinic zone at the surface. The vertical motion in the upper branch agrees with calculations by Kyle (1970) for the 500-mb vertical motion averaged from June to August. The frequent inversions near 800 mb at Lagos and Abidjan which were first noted by Hamilton and Archbold (1945) and the small values of monthly mean precipitation along the south coast of the African bulge from July to September must be the result of subsidence in the equatorward branch of the meridional circulation. Typical temperature soundings for consecutive days at Abidjan (Fig. 5.4) show that an isothermal layer or inversion with a rapid decrease of dew point occurs almost daily near 800 mb.

#### 5.4 Baroclinic Instability

Unfortunately baroclinic theory has not yet been developed for the latitudes considered in this study. The monthly mean surface temperature gradient of  $10^{\circ}\text{C}$  in  $10^{\circ}$  latitude which occurs during the African wave season is comparable to that observed in middle latitudes

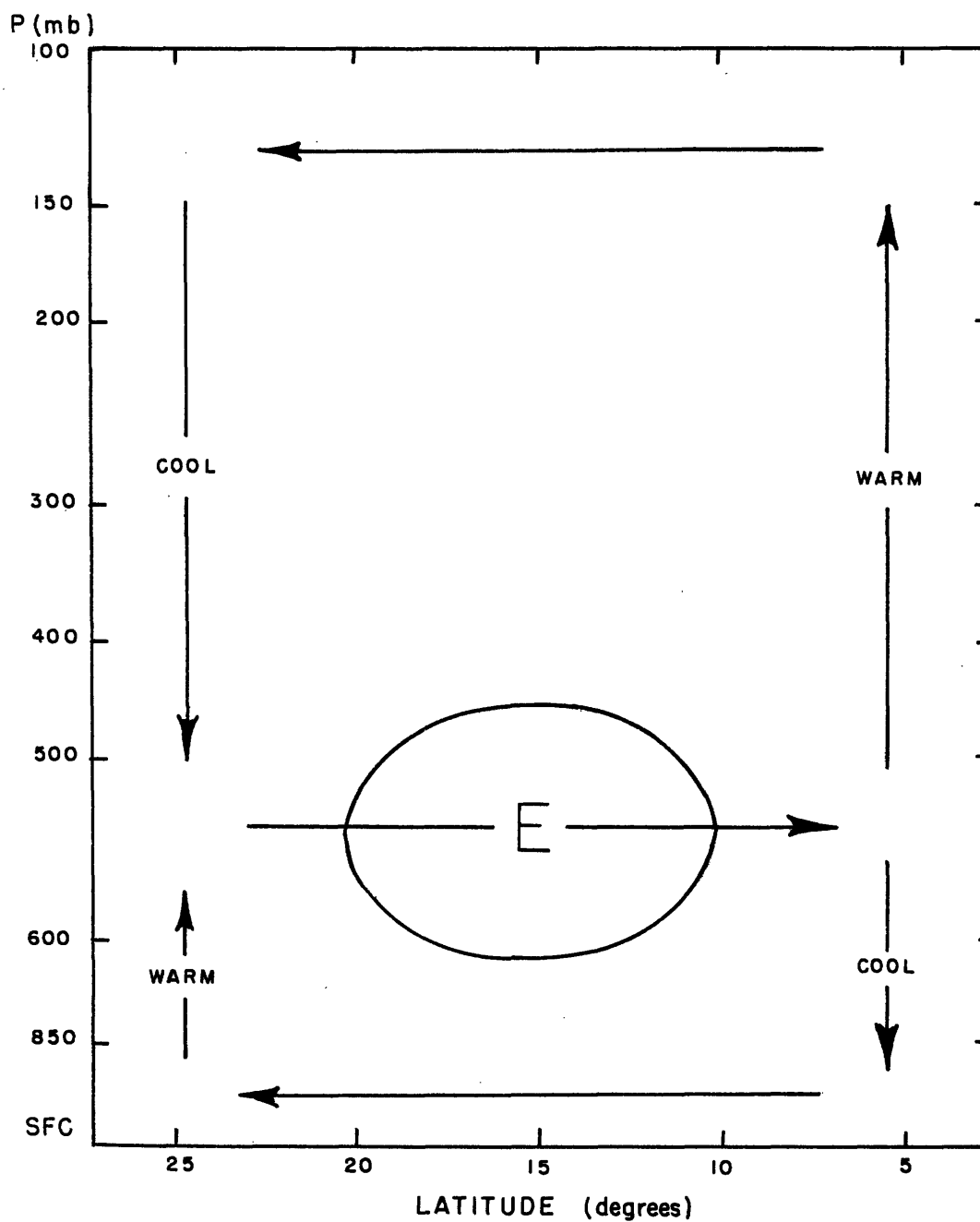


Fig. 5.3. Idealized cross section of thermally direct, ageostrophic meridional circulation and its position relative to the mid-tropospheric easterly jet.

Table 5.1

Meridional winds (m/sec) averaged from June to September for the years from 1960 to 1964, southerly winds are positive.

	<u>Khartoum</u>	<u>Ft. Lamy</u>	<u>Niamey</u>
sfc	3.4	1.2	1.4
850	0.7	0.1	0.7
700	-2.3	-2.3	-1.6
500	0.5	-1.1	-1.6
400	-0.4	-0.3	-1.4
300	0.0	0.1	-1.0
200	1.9	1.2	0.3
150	4.2	1.6	1.7
100	3.4	0.7	0.5

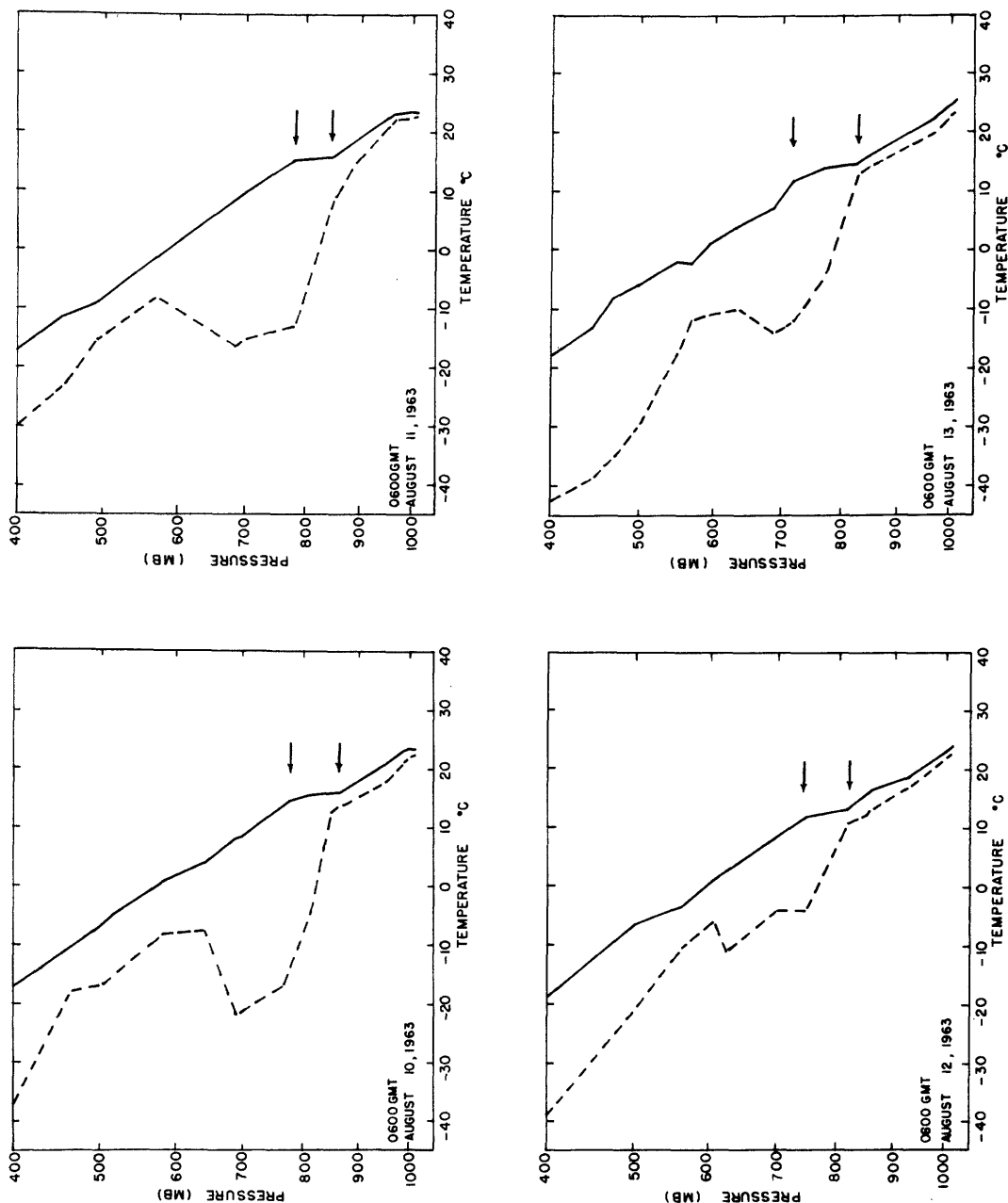


Fig. 5.4. Temperature and dew point (dashed line) soundings at Abidjan; arrows indicate upper and lower limits of stable layer near 800 mb.

during the winter; it is likely that baroclinic processes are important in such a large temperature gradient. Since the amplitude of the meridional wind of the average African wave is only 1-2 m/sec, it is unlikely that an observational study would be able to determine the magnitude of baroclinic processes in producing the kinetic energy of the waves; therefore, the role of baroclinicity in the initial generation and maintenance of these disturbances merits investigation by numerical methods.

## Chapter 6

## Discussion and Conclusion

This thesis has investigated the origin and structure of easterly waves in the lower troposphere of North Africa. Systematic use of power-spectrum and cross-spectrum analysis has shown that these tropical disturbances form over east-central Africa in the latitude band of 10-15°N and that these waves first appear near the 700-mb level. African waves are closely associated with the mid-tropospheric easterly jet (easterly wind maximum in eastern Africa) which arises in response to the strong surface baroclinic zone between the Sahara and equatorial Africa and is not part of the well-known higher-level easterly jet. The narrow latitude band of 10° in which the monthly mean temperature changes by 10°C produces a large vertical shear of the zonal wind and also creates a large horizontal shear of the zonal wind. This horizontal shear is sufficiently large that the zonal current is barotropically unstable at 700 and 500 mb. During the same season that the zonal wind is unstable, easterly waves form which have a statistically determined horizontal wavelength of 4000 km and period of 4-5 days and a synoptically observed wavelength of 2000 km and period of 3.2 days. While baroclinic processes may be important, their effect can not be determined from the data and should be investigated numerically. The African waves transport easterly momentum away from the mid-tropospheric jet, yet in this same zone the easterly flow actually increases. The source of kinetic energy for the easterly jet is undoubtedly an ageostrophic meridional

circulation (Fig. 5.3) in which warm air is rising and cool air sinking. The kinetic energy balance of this jet is quite unlike that of the mid-latitude westerly jet in which transport of momentum by eddy motions maintains the jet and a weak meridional circulation tends to decrease it.

Convection is not an important factor in the origin of these disturbances nor is the ITC directly involved since its mean position is well to the north of the main formative zone of African waves. In the zone of maximum African wave activity the magnitude and direction of the surface wind are quite uniform with the result that the horizontal shear of the surface wind is not a factor in the origin of these perturbations.

Gray (1968) investigated the global origin of tropical disturbances over the oceans for which he demonstrated that cyclonic shear of the surface wind and small values of the vertical shear of the horizontal wind are favorable factors for the formation of tropical disturbances. He concluded that large-scale frictionally forced surface convergence acting in cooperation with cumulus convection accounts for the generation of most tropical perturbations. Over North Africa, however, the shear of the horizontal wind between the surface and 600 mb is frequently greater than 15 m/sec and the horizontal shear of the surface flow is negligible. The typical environment which favors the generation of oceanic tropical disturbances is considerably different than that which produces African waves.

Spectral analysis techniques have been used to investigate easterly waves in the equatorial Pacific. Three studies of approximately the same stations but for different seasons have been published and confirm that there are fluctuations of the meridional wind in the troposphere with a period of 4-5 days.

Wallace and Chang (1969) examined disturbances in the lower troposphere from July to December 1963 and found fluctuations in the meridional wind with a period of 4-5 days which had a horizontal wavelength of approximately 3000 km and propagated toward the west. The ridge and trough axes of these easterly waves were nearly vertical with negligible phase difference from the surface to 500 mb. Although the temperature oscillations were too small to resolve, Wallace and Chang estimated that the troughs were cool and that convection was generally a maximum to the east of the trough axis.

Chang et al. (1970) studied the same region from July to December 1964, a season in which the variance of the meridional wind was nearly an order of magnitude greater than for the previous year. At Canton Island ( $3^{\circ}\text{S}$ ,  $172^{\circ}\text{W}$ ) during 1964 it was noted that the wave axis sloped rapidly toward the east with height. Farther west the vertical structure of the waves resembled that of the previous year but the amplitude was considerably larger, the period was 6-7 days and the wavelength approximately 4000 km. In the lower levels of the troposphere the easterly waves transported horizontal momentum down the gradient of mean zonal wind so that zonal kinetic energy was converted to eddy kinetic energy.



Nitta (1970a,b) spectrally analyzed time series of stations in the Pacific from April to July 1962. He concluded that there are two types of lower tropospheric wave motion with periods near four days. The first type was observed east of the international date line near the Line Islands and Canton Island. The axes of these waves tilted toward the east with height in a similar manner to that described by Chang et al. for Canton Island during the fall of 1964. He estimated that the horizontal wavelength was about 10,000 km. The second type of wave motion was found in the western Pacific with a wavelength of 5000 km and a nearly vertical trough axis. Nitta observed that the direction of the momentum transport was such as to create zonal kinetic energy at the expense of eddy kinetic energy: the opposite of the transformation computed by Chang et al. during 1964. Estimates of all energy transformations indicated that the wave motion might be driven by lateral forcing from middle latitudes in a manner similar to that suggested by Mak (1969). Nitta was unable to find any relation between the low-level disturbances in the eastern Pacific and those in the western Pacific.

These three reports present results which are difficult to combine in a single theory. At least part of the disparity may reflect lack of reliability of the statistical results due to the small length of the data samples; nevertheless, with the possible exception of the fall of 1963, there appears to be a consistent difference between the characteristics of tropospheric wave disturbances of the eastern Pacific and those of the western Pacific. The year-to-year variations of the

direction of the energy transformations and the variations of the estimates of the wavelength and period of easterly waves which have been observed in the western Pacific indicate that there may also be yearly changes in the generating mechanisms of these disturbances.

Although the period and wavelength of African waves and oceanic easterly waves of the Pacific are nearly identical, there are some consistent distinctions between the two regions. For example, the waves in the Pacific are centered on the equator in a zone of nearly uniform surface temperature while the African waves occur above a strong surface temperature gradient. Barotropic instability is essential to the initiation of tropical disturbances over Africa during each year from 1960 to 1964, yet Wallace and Chang (1969) found little or no horizontal shear during 1964 when wave activity in the Pacific was considerably enhanced. They conclude that lateral shear inhibits the Pacific waves. In addition convection may be important to the maintenance of the Pacific easterly waves since spectral analysis shows a peak of mean relative humidity at 4-5 days but convection is not a significant factor in the generation of African waves.

It is important to note that Wallace and Chang, Chang et al., and Nitta have not isolated the origin of tropical disturbances but have studied propagating waves which formed outside of their data network. Many of their conclusions concerning energy transformations are, therefore, relevant only to the maintenance of these waves.

While surface temperatures in each of the other equatorial land masses reach a maximum at latitudes approximately  $15-25^{\circ}$  poleward of

the equator, the temperature gradients are considerably less than that found over Africa. Exclusive of North Africa, Australia is the most likely place for surface temperature gradients sufficiently large to produce a barotropically unstable current in the middle troposphere, but the existing data network is not capable of showing it. Since tropical disturbances form in the surface easterlies both to the east and the west of Australia (see e.g. Gray, 1968), the cyclonic shear of the zonal wind in the northern part of Australia during the southern hemisphere summer may merely enhance the development of pre-existing disturbances rather than cause the formation of new waves.

There are other land areas which merit investigation as possible influences on the development of tropical disturbances. These include the suppression of tropical perturbations north of South America in the eastern Caribbean and the enhanced development of disturbances in the eastern Pacific south of Central America.

### Acknowledgements

This thesis culminates a long period of formal study during which many people have made direct and indirect contributions to this study. The author is particularly appreciative of the efforts of his friend and teacher Professor Frederick Sanders for his encouragement and valuable advice throughout this research and for his help in preparing the final manuscript. Thanks are also extended to Professor Jule G. Charney and Professor Edward N. Lorenz for their helpful comments and suggestions.

This study is an extension of the careful study of African waves by Dr. Toby N. Carlson of the National Hurricane Research Laboratory. His enthusiasm for understanding the role of African waves in the development of tropical cyclones in the North Atlantic helped to formulate the ideas which led to this thesis.

The data for the upper-air cross sections were processed by Professor Reginald E. Newell under contract No. AF(30-1)2241 with the U.S. Atomic Energy Commission. The numerical computations were made at the M.I.T. Information Processing Center and the research was sponsored by grants E-22-37-(69)G and E-22-37-(70)G from the Environmental Science Services Administration.

Special thanks to Miss Anna K. Corrigan for plotting the African maps, to Miss Isabel Kole for drafting the figures and to Mrs. Marie Gabbe for typing the manuscript.

## Appendix

The method of analysis in this study closely parallels the technique of Bendat and Piersol (1966). For data values  $\{x_m\}$ ,  $m = 1, 2, \dots, N$ , which are obtained by sampling at fixed intervals  $\Delta t$  from a stationary series with zero mean, the estimated autocorrelation function is defined at lag  $j$  by

$$R(j) = \frac{1}{N-j} \sum_{m=1}^{N-j} x(m) x(m+j) \quad j = 0, 1, \dots, m$$

where  $j$  is the lag number and  $m$  is the maximum lag number. The power spectral density function is the Fourier transform of the autocorrelation function. For a continuous covariance function  $R(\tau)$  the power spectrum  $E(\omega)$  is given by

$$E(\omega) = \frac{2}{\pi} \int_0^{\infty} R(\tau) \cos \omega \tau d\tau$$

where  $\omega = 2\pi f$ ,  $f$  is frequency in cycles per unit time and  $\tau$  is delay time. When  $R(\tau)$  is obtained by discrete sampling at intervals  $\Delta t$ , the estimate of the power spectral density function is

$$G(f) = 2 \Delta t \left[ R(0) + 2 \sum_{j=1}^{m-1} R(j) \cos\left(\frac{\pi j f}{f_c}\right) + R(m) \cos\left(\frac{\pi m f}{f_c}\right) \right]$$

where  $f_c = \frac{1}{2\Delta t}$  is the highest resolvable frequency in the

discrete record and  $f$  need be evaluated only at the frequencies

$$f = \frac{k f_c}{m} \quad k = 0, 1, \dots, m$$

The number of lags involved in the autocorrelation curve is generally not sufficient to insure that  $R(m)$  approach zero. In order to minimize the effects of a non-zero  $R(m)$ , the Hanning method of smoothing is applied to the  $G(f)$

$$\bar{G}(0) = 0.5 G(0) + 0.5 G\left(\frac{f_c}{m}\right)$$

$$\bar{G}\left(\frac{k f_c}{m}\right) = 0.25 G\left(\frac{(k-1) f_c}{m}\right) + 0.5 G\left(\frac{k f_c}{m}\right) + 0.25 G\left(\frac{(k+1) f_c}{m}\right)$$

$$\bar{G}(f_c) = 0.5 G\left(\frac{(m-1) f_c}{m}\right) + 0.5 G(f_c)$$

The  $\bar{G}\left(\frac{k f_c}{m}\right)$  are the desired estimates of the power spectral density.

While the power spectrum yields information concerning the distribution of energy as a function of frequency for a single time series, cross-spectrum analysis determines the relationship between two or more different time series. Just as the power spectrum is the Fourier transform of the autocorrelation function, the cross spectrum is the transform of the cross-correlation function. The cross-correlation function, however, is not generally symmetric so that odd terms as well as even terms are required to represent it. The cross-correlation function is defined by

$$\left. \begin{aligned} R_{xy}(j) &= \frac{1}{N-j} \sum_{m=1}^{N-j} x(m) y(m+j) \\ R_{yx}(j) &= \frac{1}{N-j} \sum_{m=1}^{N-j} y(m) x(m+j) \end{aligned} \right\} j = 0, 1, \dots, m$$

The even and odd parts of the cross-correlation function are

$$A(j) = \frac{1}{2} [R_{xy}(j) + R_{yx}(j)]$$

$$B(j) = \frac{1}{2} [R_{xy}(j) - R_{yx}(j)]$$

For the continuous case the cross spectral density function is

$$E_{xy} = C_{xy}(\omega) + i Q_{xy}(\omega)$$

where

$$C_{xy}(\omega) = \frac{2}{\pi} \int_0^{\tau_m} A(\tau) \cos \omega \tau d\tau$$

$$Q_{xy}(\omega) = \frac{2}{\pi} \int_0^{\tau_m} B(\tau) \sin \omega \tau d\tau$$

$C_{xy}(\omega)$  is the co-spectral density function and  $Q_{xy}(\omega)$  is the quadrature spectral density function. The discrete approximations of  $C_{xy}(\omega)$  and  $Q_{xy}(\omega)$  are

$$C_{xy}(f) = 2\Delta t \left[ A(0) + 2 \sum_{j=1}^{m-1} A(j) \cos\left(\frac{\pi j f}{f_c}\right) + A(m) \cos\left(\frac{\pi m f}{f_c}\right) \right]$$

$$Q_{xy}(f) = 2\Delta t \left[ 2 \sum_{j=1}^{m-1} B(j) \sin\left(\frac{\pi j f}{f_c}\right) + B(m) \sin\left(\frac{\pi m f}{f_c}\right) \right]$$

and are evaluated at  $f = \frac{kf_c}{m}$ ;  $k = 0, 1, \dots, m$ . For smooth estimates of  $C_{xy}(f)$  and  $Q_{xy}(f)$  the Hanning method is applied in a similar manner to that used for the power spectrum. The magnitude of the cross spectral density function is

$$|\bar{G}_{xy}(f)| = [\bar{C}_{xy}^2(f) + \bar{Q}_{xy}^2(f)]^{1/2}$$

The phase lag for frequencies in time series  $\{y\}$  relative to  $\{x\}$  is given by

$$\bar{\theta}_{xy}(f) = \tan^{-1} \left[ \frac{\bar{Q}_{xy}(f)}{\bar{C}_{xy}(f)} \right]$$

The coherence is a measure of the fraction of the variance in  $\{x\}$  that can be specified by  $\{y\}$  for each frequency

$$\text{coh}_{xy}(f) = \frac{|\bar{G}_{xy}(f)|^2}{\bar{G}_x(f) \bar{G}_y(f)}$$



## Bibliography

- Arnold, J.E., 1966: Easterly wave activity over Africa and in the Atlantic with a note on the Intertropical Convergence Zone during early July 1961. SMRP Report No. 65, Dept. of Geoph. Sci., University of Chicago, 23 pp.
- Atkinson, G.D., and J.C. Sadler, 1970: Mean-cloudiness and gradient-level-wind charts over the tropics, Volume II. Technical Report 215, Air Weather Service, United States Air Force.
- Bates, J.R., 1969: Dynamics of disturbances on the Intertropical Convergence Zone. Ph.D. Thesis, M.I.T. Dept. of Meteor., 203 pp.
- Bendat, J.S., and A.G. Piersol, 1966: Measurement and Analysis of Random Data. New York, Wiley, 390 pp.
- Carlson, T.N., 1969a: Synoptic histories of three African disturbances that developed into Atlantic hurricanes. Mon. Wea. Rev., 97, 256-276.
- Carlson, T.N., 1969b: Some remarks on African disturbances and their progress over the tropical Atlantic. Mon. Wea. Rev., 97, 716-726.
- Chang, C.-P., V.F. Morris, and J. M. Wallace, 1970: A statistical study of easterly waves in the western Pacific: July-December 1964. J. Atmos. Sci., 27, 195-201.
- Denney, W.J., 1969: The eastern Pacific hurricane season of 1968. Mon. Wea. Rev., 97, 207-224.
- Dunn, G.E., 1940: Cyclogenesis in the tropical Atlantic. Bull. Amer. Met. Soc., 21, 215-229.
- Eldridge, R.H., 1957: A synoptic study of West African disturbance lines. Quart. J. Roy. Met. Soc., 83, 303-314.
- Frank, N.L., 1969: The "Inverted-V" cloud pattern - an easterly wave? Mon. Wea. Rev., 97, 130-140.
- Frank, N.L., 1970: Atlantic tropical systems of 1969. Mon. Wea. Rev., 98, 307-314.
- Gray, W.M., 1968: Global view of the origin of tropical disturbances and storms. Mon. Wea. Rev., 96, 669-700.
- Hamilton, R.A., and J.W. Archbold, 1945: Meteorology of Nigeria and adjacent territory. Quart. J. Roy. Met. Soc., 71, 231-262.

- Hubert, H., 1939: Sur l'origine africaine d'un cyclone tropical dévastateur dans la région de New York, C.-R. des séances de l'Acad. des Sciences, Paris, 208, p. 456. Summarized by C.F. Brooks, 1940: Hubert on the African origin of the hurricane of 1938. Trans. Amer. Geophys. Union, 21, 251-253.
- Kidson, J.W., 1968: The general circulation of the tropics. Ph.D. Thesis, M.I.T., Dept. of Meteor., 205 pp.
- Kyle, A.C., 1970: Longitudinal variations of large-scale vertical motion in the tropics. S.M. Thesis, M.I.T., Dept. of Meteor., 56 pp.
- Lenhard, R.W., 1970: Accuracy of radiosonde temperature and pressure-height determination. Bull. Amer. Met. Soc., 51, 842-846.
- Lipps, F.B., 1970: Barotropic stability and tropical disturbances. Mon. Wea. Rev., 98, 122-131.
- Mak, M.K., 1969: Laterally driven stochastic motions in the tropics. J. Atmos. Sci., 26, 41-64.
- Manabe, S., J.L. Holloway, Jr., and H.M. Stone, 1970: Tropical circulation in a time-integration of a global model of the atmosphere. J. Atmos. Sci., 27, 580-613.
- Nitta, T., 1970a: Statistical study of tropospheric wave disturbances in the tropical Pacific region. J. Met. Soc. Japan, 48, 47-60.
- Nitta, T., 1970b: On the role of transient eddies in the tropical troposphere. J. Met. Soc. Japan, 48, 348-359.
- Nitta, T., and M. Yanai, 1969: A note on barotropic instability of the tropical easterly current. J. Met. Soc. Japan, 47, 127-130.
- Ooyama, K., 1969: Numerical simulation of the life cycle of tropical cyclones. J. Atmos. Sci., 26, 3-40.
- Palmer, C.E., 1952: Tropical meteorology. Quart. J. Roy. Meteor. Soc., 78, 126-163.
- Panofsky, H.A., and G.W. Brier, 1958: Some Applications of Statistics to Meteorology. University Park, The Pennsylvania State University, 224 pp.
- Piersig, W., 1936: Schwankungen von Luftdruck und Luftbewegung sowie ein Beitrag zum Wettergeschehen in Passatgebiet des ostlichen Nordatlantischen Ozeans, 54. Parts II and III have been translated and printed, 1940: The cyclonic disturbances of the subtropical eastern North Atlantic. Bull. Amer. Met. Soc., 25, 2-17.

- Regula, H., 1936: Druckschwankungen und Tornados an der Westkuste von Afrika. Annalen der Hydrographie und Maritimen Meteorologie, 107-111.
- Riehl, H., 1945: Waves in the easterlies and the polar front in the tropics. Dept. Meteor., Univer. Chicago, Misc. Rept., No. 17, 79 pp.
- Schove, D.J., 1946: A further contribution to the meteorology of Nigeria. Quart. J. Roy. Met. Soc., 72, 105-110.
- Simpson, R.H., N. Frank, D. Shideler, and H. Johnson, 1968: Atlantic tropical disturbances, 1967. Mon. Wea. Rev., 96, 251-259.
- Simpson, R.H., N. Frank, D. Shideler, and H. Johnson, 1969: Atlantic tropical disturbances of 1968. Mon Wea. Rev., 97, 240-255.
- U.S. Navy, Chief of Naval Operations, 1955: Marine Climatic Atlas of the World, Volume I, North Atlantic Ocean. NAVAER 50-1C-528. Washington: Government Printing Office.
- World Weather Records, 1951-1960, Vol. 5, 1968: U.S. Department of Commerce, Washington, D.C., 545 pp.
- Wallace, J.M., and C.-P. Chang, 1969: Spectrum analysis of large-scale wave disturbances in the tropical lower troposphere. J. Atmos. Sci., 26, 1010-1025.
- Yanai, M., 1961: Dynamical aspects of typhoon formation. J. Met. Soc. Japan, 39, 282-309.
- Yanai, M. and T. Maruyama, 1966: Stratospheric wave disturbances propagating over the equatorial Pacific. J. Meteor. Soc. Japan, 44, 291-294.
- Yania, M., T. Maruyama, T. Nitta, and Y. Hayashi, 1968: Power spectra of large-scale disturbances over the tropical Pacific. J. Meteor. Soc. Japan, 46, 308-323.

## Biographical Sketch

The author was born on August 5, 1941, in Reading, Massachusetts. He attended Reading public schools and in September 1959 entered Harvard College where he studied engineering and physics. While an undergraduate the author was undecided about a future profession; however, nature's infrequent displays of power in the form of snowstorms, thunderstorms and hurricanes and the shortcomings of many local weather forecasts stimulated his interest in meteorology and convinced him that the atmospheric sciences would be an exciting area for further study. After gaining his A.B. from Harvard in June of 1963, the author entered the Department of Meteorology at M.I.T. where he received his S.M. in 1966. From 1967 to 1969 he spent more than a year at the National Hurricane Research Laboratory in Miami while working on a barotropic hurricane track forecasting model with Professor Frederick Sanders. It was in Miami that he became interested in the problem of African waves. His graduate studies were aided by research assistantships under the direction of Dr. Pauline M. Austin and Professors Jule G. Charney and Frederick Sanders.